2020-12-08

Novel Analytical Method for Trace Level Quantification of Disinfection By-Products in Recycled Wastewaters

Ortega, Alejandro Rene

UNIVERSITY OF CALGARY

Novel Analytical Method for Trace Level Quantification of Disinfection By-Products in Recycled Wastewaters

by

Alejandro Rene Ortega

A THESIS

SUBMITTED TO THE FACULTY OF GRADUATE STUDIES

IN PARTIAL FULFILMENT OF THE REQUIREMENTS FOR THE

DEGREE OF MASTER OF SCIENCE

GRADUATE PROGRAM IN CHEMISTRY

CALGARY, ALBERTA

DECEMBER, 2020

Abstract

The work of this thesis quantifies and characterizes unregulated priority disinfection by-products (DBPs) in a full-scale potable wastewater reuse treatment plant. DBPs are small organic molecules formed from the reaction between natural organic matter (NOM) and disinfectants. Unregulated DBPs display genotoxic, cytotoxic and potentially carcinogenic properties to humans. Wastewater reuse is an area of growing interest as freshwater sources are being depleted due to increasing human population and climate change. Secondary effluent treated with microfiltration (UF), ozone, and reverse osmosis waters were disinfected to observe the change in DBP composition throughout various stages of the treatment train process.

First, a novel multiple reaction monitoring (MRM) method was developed on a gas chromatography – triple quadrupole mass spectrometer (GC-MS/MS) that quantifies 25 DBPs formed from chlorinated and chloraminated wastewater effluents. The order of optimization of each DBP class involved the determination of chemical transitions, collision energies, dwell times, time segments and determination of method detection limits. The optimization of these parameters led to a highly sensitive quantification method for the DBPs found in this method. Method detection limits ranged from 2.0 - 68.9 ng/L.

Next, a liquid – liquid extraction (LLE) method for sample analysis was modified to account for the large increase in sensitivity that comes with a triple quadrupole. MS/MS instruments are highly advantageous because of the selection of specific chemical transitions for quantification. This specificity results in precise quantification due to the large signal to noise ratio of each chemical fragment at trace levels. The LLE method was

reduced 10 fold in terms of time, reagents, and sample volume compared to published methods.

The last part of this work looked at the DBP composition of each water matrix across three seasons of the year. Specifically, waters were sampled in fall, winter, and summer to observe how the change in precursors affected DBP formation.

.

Preface

Portions of Chapter 2 and Chapter 3 are part of: Ortega-Hernandez, A.; Acayaba, R.; Verwold, C; Montagner, C.; Kimura S. Y. Emerging Disinfection By-product Quantification Method for Wastewater Reuse: Trace Level Assessment using Tandem Mass Spectrometry, submitted to the journal of Environmental Science: Water Research & Technology.

Acknowledgment

I would like to thank Dr. Susana Kimura-Hara, my MSc and 4th year undergraduate supervisor. When I was about to graduate with my BSc from the University of South Carolina, Susana asked me to follow her for my graduate degree in Canada. I was resistant to the idea because I did not feel smart enough to complete research at the graduate level. Describing Susana as supportive would be an understatement. It has been a privilege working for her, and I am glad I pushed through under her mentorship.

I would like to extend a huge thanks to my committee members, Dr. Kevin Thurbide, Dr. Gopal Achari, and Dr. Jeffrey Van Humbeck for all the helpful advice and constructive criticism received in my annual meetings. I am also thankful for the Eyes High Doctoral Scholarship I received during my first two years.

I am grateful for the Kimura-Hara group. Throughout my graduate program I was able to make long – lasting friendships from the lab. Specifically, I would like to acknowledge Thilina Jayawardana, Chad Verwold, and Jillian Murakami. Thilina, thank you for always lending a listening ear and supportive feedback. Chad, I am grateful this degree program gifted me a friend like yourself, but also a colleague who provided insightful feedback when I would verbalize my thought processes concerning my lab work.

During my time in the Kimura-Hara group we had Raphael Acayaba from UNICAMP in Campinas, Brazil as a visiting student. During his time at the Kimura-Hara lab we became close friends and colleagues. Raphael helped me during the LLE optimization and with most of the validation work for the analytical method. He is a dear friend who helped me so much during his time in the Kimura-Hara lab.

I would like to acknowledge Jill. Jill, in you I have found a mentor, friend, the big sister I never had, and a teacher both in lab and life practices. Thank you so much for all the help you extended me during the formation potential tests.

A huge thanks to Carlos Ortega, Citlali Ortega, Luciano Ortega, my niece Silvana Ortega, and Santiago Ortega. I am so blessed to have such an amazing brother and sister in-law. Thank you for giving me my nephews. Silvana's FaceTimes are priceless for me.

Lastly, I would like to thank my partner Jack Novovic and my dogs Bisquick and Basil. Knowing I had a family to come home to was always comforting and reassuring. I cannot thank you enough for all the laughs, good times, and support I received during this challenging endeavour that is graduate school. I love you guys so much and I am truly blessed to have you in my life.

To my mom, my brother, my dad, and my partner Jaksa Novovic

Table of Contents

List of Tables

List of Figures

List of Symbols, Abbreviations and Nomenclature

111TCP	1,1,1-Trichloropropanone
1133TeCP	1,1,3,3-Tetrachloropropanone
113TCP	1,1,3-Trichloropropanone
11DCP	1,1-Dichloropropanone
13DCP	1,3-Dichloropropanone
1B11DCP	1-Bromo-1,1-dichloropropanone
AC	Activated carbon
ACWA	Advancing Canadian Wastewater Assets
NH_3	Ammonia
avg	Average
$AV_{PeakArea}$	Average peak area
BAN	Bromoacetonitrile
BCAN	Bromochloroacetonitrile
BCIM	Bromochloroiodomethane
BCNM	Bromochloronitromethane
BDCAld	Bromodichloroacetaldehyde
BDIM	Bromodiiodomethane
Br^-	Bromide
x	By
C	Carbon
CO_2	Carbon Dioxide
cm	Centimeter
Cl^-	Chloride

CDFW	Chlorine Demand Free Water
CAN	Chloroacetonitrile
CDIM	Chlorodiiodomethane
CE	Collision energy
°C	Degree Celsius
DBAN	Dibromoacetonitrile
DBCAld	Dibromochloroacetaldehyde
DBIM	Dibromoiodomethane
DBNM	Dibromonitromethane
DCAN	Dichloroacetonitrile
DCIM	Dichloroiodomethane
DCNM	Dichloronitromethane
DC	Direct current
DBP	Disinfection By-product
DOC	Dissolved organic carbon
EfOM	Effluent organic matter
eV	Electron volt
et al.,	Et alia (and others)
Exp	Experiment
GC	Gas chromatography
HAA	Haloaceticacids
HALD	Haloaceticaldehydes
HAN	Haloacetonitriles

HKT	Haloketones
HNM	Halonitromethanes
HOCl	Hypochlorous acid
ID	Internal diameter
I^-	Iodide
IAN	Iodoacetonitrile
TIM	Iodoform
I-THM	Iodo-Trihalomethanes
LLE	Liquid – liquid extractions
L	Litre
m/z	Mass to charge ratio
MDLs	Method detection limits
UF	Microfiltration
µg	Microgram
µL	Microliter
mg	Milligram
mL	Millilitre
mM	Millimolar
ms	Milliseconds
min	Minutes
NH_2Cl	Monochloramine
MRM	Multiple reaction monitoring
ng	Nanogram

NOM	Natural organic matter
N_2	Nitrogen gas
O_3	Ozone
ppb	Parts per billion
ppm	Parts per million
ppt	Parts per trillion
pw	Peak width
%	Percent
q	Qualitative ion
Q	Quantitative ion
RF	Radio frequency
RSD	Relative standard deviation
R.T.	Retention time
RO	Reverse osmosis
n	Sample size
$SD_{PeakArea}$	Standard deviation of the average peak area
MS/MS	Tandem mass spectrometer/ Triple quadrupole
TN	Total nitrogen
TOBr	Total organic bromide
TOC	Total organic carbon
TOCl	Total organic chloride
TOI	Total organic iodide
TBAld	Tribromoacetaldehyde

TCAN	Trichloroacetonitrile
THM	Trihalomethane
$t_{N-1,1-\alpha=0.99}$	t-test value at the 99th percentile
UFC	Uniform formation conditions

Chapter 1: Introduction

1.1 Water Treatment and Disinfection By-products (DBPs)

DBPs result when disinfectants are added to water in order to treat it for potable consumption. Typically, these chemicals are small organic and inorganic compounds formed as the result of disinfectants reacting with natural organic matter (NOM) and inorganic salts present in surface (rivers and lakes) and groundwater. Conventional water treatment involves multiple steps including pre-screening, flocculation, sedimentation, filtration, disinfection and distribution to remove particles and harmful pathogenic microorganisms. Below is a brief description of how drinking water is treated in Calgary, Alberta.

The City of Calgary follows a treatment process similar to the general schematic of Figure 1-1. Initially, river water (influent) is passed through a debris screen to prevent the uptake of any aquatic organisms or larger debris. A coagulant is added in the flocculation tank to help create flocs of dissolved matter that are separated from the aqueous phase. Clarified water passes to a tank where the initial chlorination takes place. This step is where a disinfectant (i.e., chlorine) can react with dissolved NOM to form DBPs while effectively destroying microorganisms that are harmful to the human body. [1, 2] Following the initial chlorination step, the water then flows through sand filtration beds to remove any remaining particles. The final step involves one final chlorination that is dosed to prevent any further outbreaks during the distribution of the finished waters.

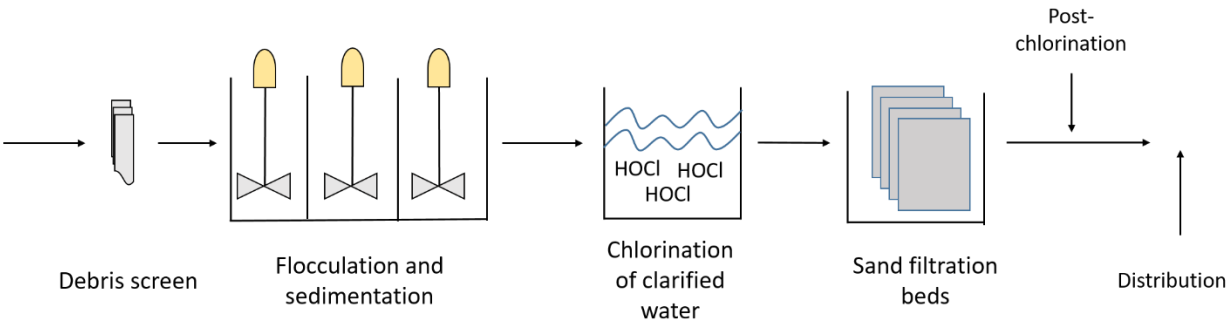

Figure 1-1: General schematic of a drinking water treatment train

Treating wastewater involves a different water treatment process. The differences between the treatments is due to the different contaminants present in the matrix. Specifically, this work aims to evaluate the efficiency of DBP precursor removal at each treatment step. This information is valuable for potable reuse plants and drinking water treatment plants that experience wastewater impacted source waters.

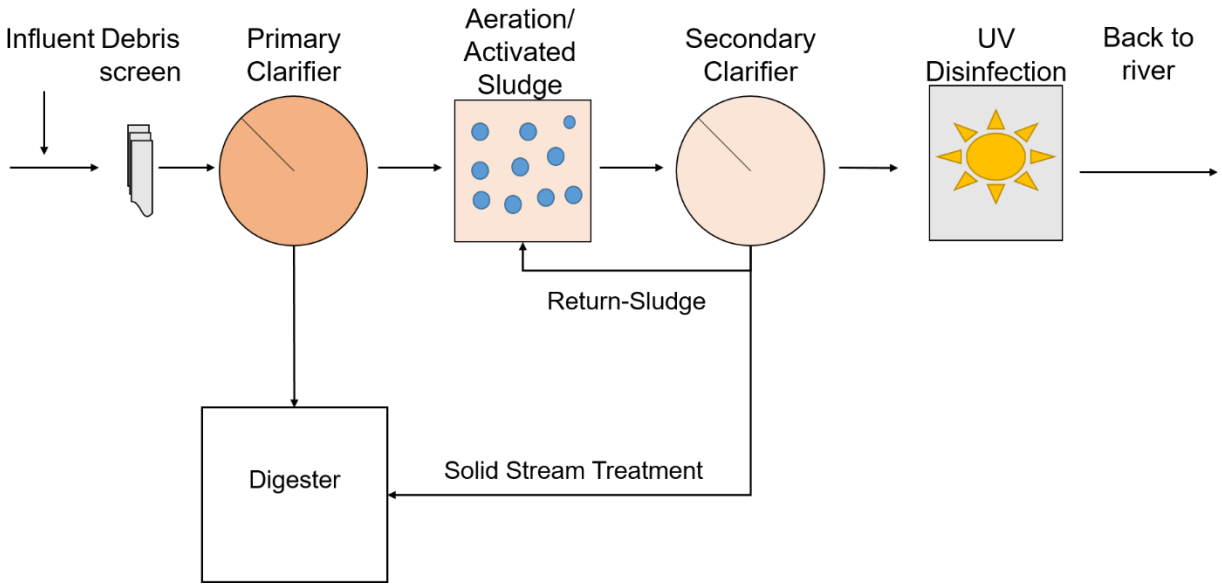

Figure 1-2: General schematic of a Wastewater Treatment Plant

Figure 1-2 is a schematic that illustrates how wastewater is treated in order to be reintroduced into the environment in a safe manner. Initially, wastewater intake is taken from a collection system where it is passed through a series of screens to remove debris

that may damage the treatment train. Once filtered, water is passed onto the primary clarifier where the wastewater is held for about three hours in order for the solids to settle at the bottom, and lipids and oils rise to the top. Solids are then removed and further processed in the solid – stream treatment train process. [2, 3] Once lipids are skimmed off, the effluent is passed to an aerated tank, where microbial digestion occurs to further breakdown organic matter and nutrients present in the effluent. The wastewater is then passed into the secondary clarifier where remaining solids settle to the bottom. A portion of the bioactive sludge is returned to the aeration tank and the rest is subjected to the solid stream treatment process. The final step typically involves microbial inactivation. UV disinfection is a disinfection method in which microbes are passed through a UV lamp that damages the microbial DNA structure, thereby prevent microbial reproduction. [2, 3]

1.2 DBP Toxicity

Upon the discovery of DBPs in 1974, more than 600 DBPs have been identified in disinfected waters. [4] Of these 600 DBPs, only about 100 have undergone a systematic cyto- and genotoxicity analysis. [5] DBPs may damage the cell's metabolic activity (cytotoxicity) and/or damage the cell's DNA sequencing (genotoxicity), leading to cell death or DNA strand breaks. Currently, Canada only monitors 12 DBPs including trihalomethanes (THMs) and haloaceticacids (HAAs). However, THMs and HAAs have shown to possess some of the lowest cytotoxic response in Chinese hamster ovary (CHO) cell lines compared to other unregulated DBPs. [6, 7] Typically, toxicity increases based on the substituted halogen following the general trend of I (most toxic) >> Br >Cl (least toxic).

Although regulated DBPs are documented to induce CHO cell death, unregulated nitrogen-containing DBPs (N-DBPs) have shown to be the main cytotoxic and genotoxic drivers within DBPs. Unregulated N-DBPs such as haloacetonitriles, haloacetamides, and halonitromethanes have gained increasing attention as they tend to show an increased risk in cytotoxic and genotoxic damage in CHO cells. N-DBPs may form at higher concentrations when oxidants react with effluent organic matter (EfOM) and dissolved organic nitrogen (DON) in wastewater matrices. [8-11] However, most studies have all focused on only one chemical class or a small subset of N-DBPs. In this work we aim to disinfect and characterize five classes of high priority DBPs, mostly nitrogen containing, with one simultaneous analytical method.

Figure 1-3A below shows the concentration at which 50% of cell death occurs of the CHO cell line for THMs, also known as LC_{50} values.[12] Wagner and Plewa compared

the LC_{50} values of unregulated DBPs and found that HANs were 2-3 orders of magnitude less compared to THMs (Figure 1-3B). Figure 1-3B only shows HANs, however several unregulated classes were studied. Therefore, it is important to evaluate unregulated DBPs as they have been shown to be more toxic than regulated DBPs.

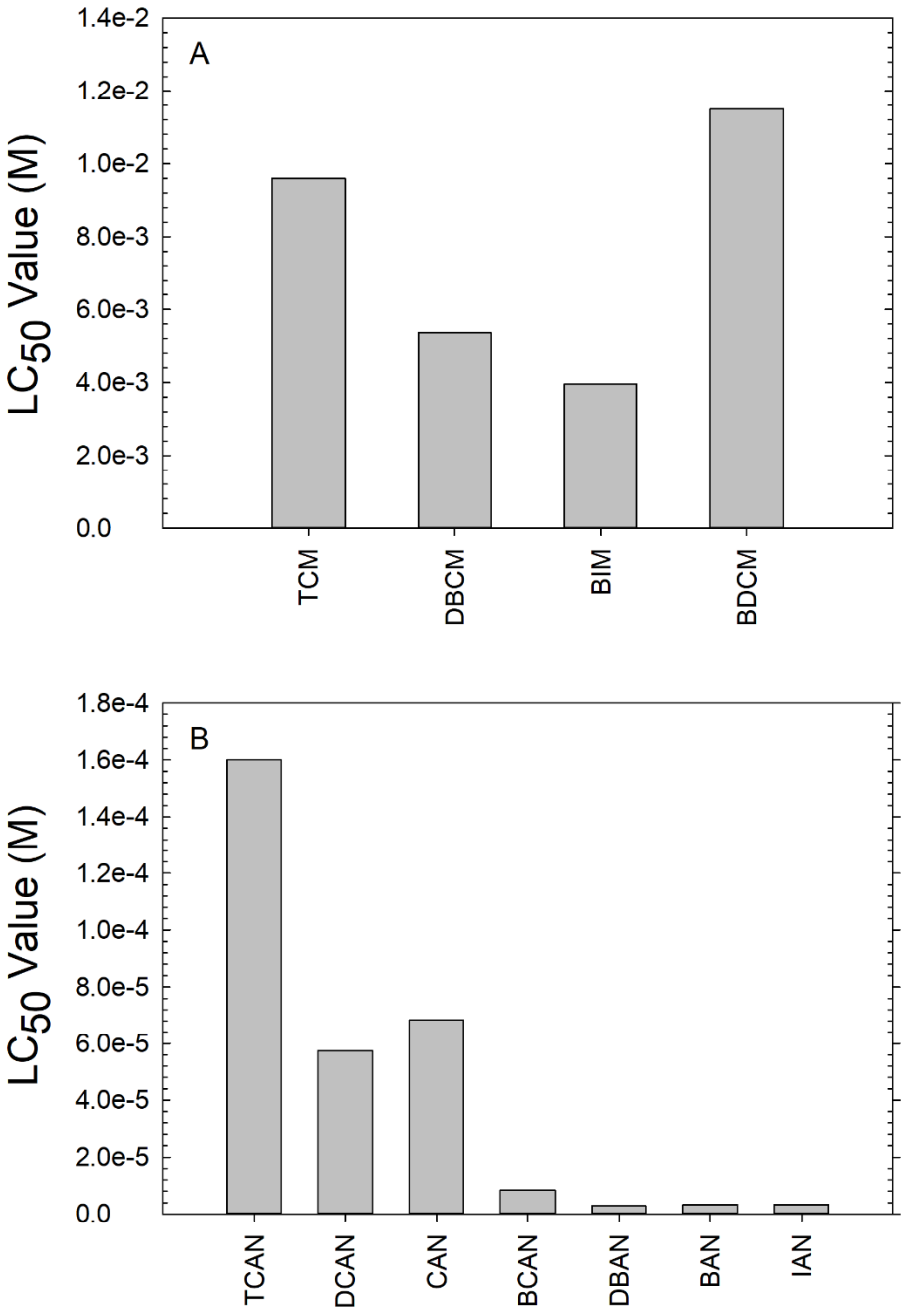

Figure 1-3: Cytotoxic LC_{50} Values on Chinese Hamster Ovary (CHO) Cell Line of regulated DBPs **(A)**, and unregulated HANs **(B)**. [12]

1.3 Chemical Disinfection

There are four major chemical disinfectants and UV light that are used in water treatment worldwide. In Canada, free chlorine (HOCl), and combined chlorine (NH_2Cl) are the most commonly used in water treatment facilities. [13] Two other disinfectants that may also be used are ozone (O_3) and chlorine dioxide (ClO_2). Each disinfectant may react with organic matter to produce different by-products as shown in Table 1-1. The following section briefly describes the differences between the aforementioned chemical disinfectants.

Chlorination is the most widely used disinfectant worldwide.[14] HOCl was the disinfectant associated with the first identified DBPs in the early 1970s. [2] Health Canada implemented guidelines for a maximum contaminant level (MCL) for the THM and HAA clasess.[15] Monitored THMs and HAAs include chloroform ($CHCl_3$), bromodichloromethane ($CHBrCl_2$), dibromochloromethane ($CHBr_2Cl$), bromoform ($CHBr_3$), monochloroacetic acid (MCA), dichloroacetic acid (DCA), trichloroacetic acid (TCA), monobromoacetic acid (MBA), and dibromoacetic acid (DBA). [2] Health Canada imposed an total concentration for THMs and HAAs of 0.10, 0.08 mg/L, respectively. [15, 16] Although THMs and HAAs were the first identified DBP classes, resulting in their monitoring, there are many other DBPs that may form during chlorination as shown in Table 1-1. DBP speciation is dependent on composition of source waters and water treatment processes.[2] For some water treatment facilities, DBP regulations were difficult to comply while also providing an adequate residual concentration in the distribution

system. Therefore, a strategy that was used involved switching to combined chlorine which produces less THMs and HAAs. [2]

Table 1-1: DBPs formed from common chemical disinfection methods[17]

Disinfectant	Organohalogen (DBPs)	Inorganic DBPs	Non-halogenated DBPs
Chlorine (Cl_2/HOCl)	Trihalomethanes Haloacetic Acids Haloacetonitriles Halonitromethanes Iodo-Trihalomethanes Haloketones	Chlorate	Aldehydes Alkanic acids Benzene Carboxylic Acids
Chloramines (NH_2Cl or $NHCl_2$)	Cyanogen Halides Haloacetamides Haloacetonitriles Halonitromethanes Organic chloramines	Nitrite Nitrate Chlorate Hydrazine	Aldehydes Ketones Nitrosodimethylamine
Ozone (O_3)	Bromoform	Chlorate Iodate Bromate	Aldehydes Ketones Ketoacids Carboxylic Acids
Chlorine Dioxide (ClO_2)	-	Chlorite Chlorate	-

Combined chlorine or chloramination is formed by combining HOCl and ammonia to produce chloramines as shown in Equations 1-1 to 1-4. It is important to understand how chloramines can form when HOCl is added to water in the presence of ammonia.

$$NH_{3(aq)} + HOCl_{(aq)} \rightarrow NH_2Cl_{(aq)} + H_2O_{(aq)}$$

Equation 1-1[18]

$$NH_2Cl_{(aq)} + HOCl_{(aq)} \rightarrow NHCl_{2(aq)} + H_2O_{(aq)}$$

Equation 1-2[3]

$$NHCl_{2\,(aq)} + HOCl_{(aq)} \rightarrow NCl_{3(aq)} + H_2O_{(aq)}$$

Equation 1-3[3]

$$2NH_2Cl_{(aq)} + HOCl_{(aq)} \rightarrow N_{2(g)} + H_2O_{(aq)} + 3H^+_{(aq)} + 3Cl^-_{(aq)}$$

Equation 1-4[3]

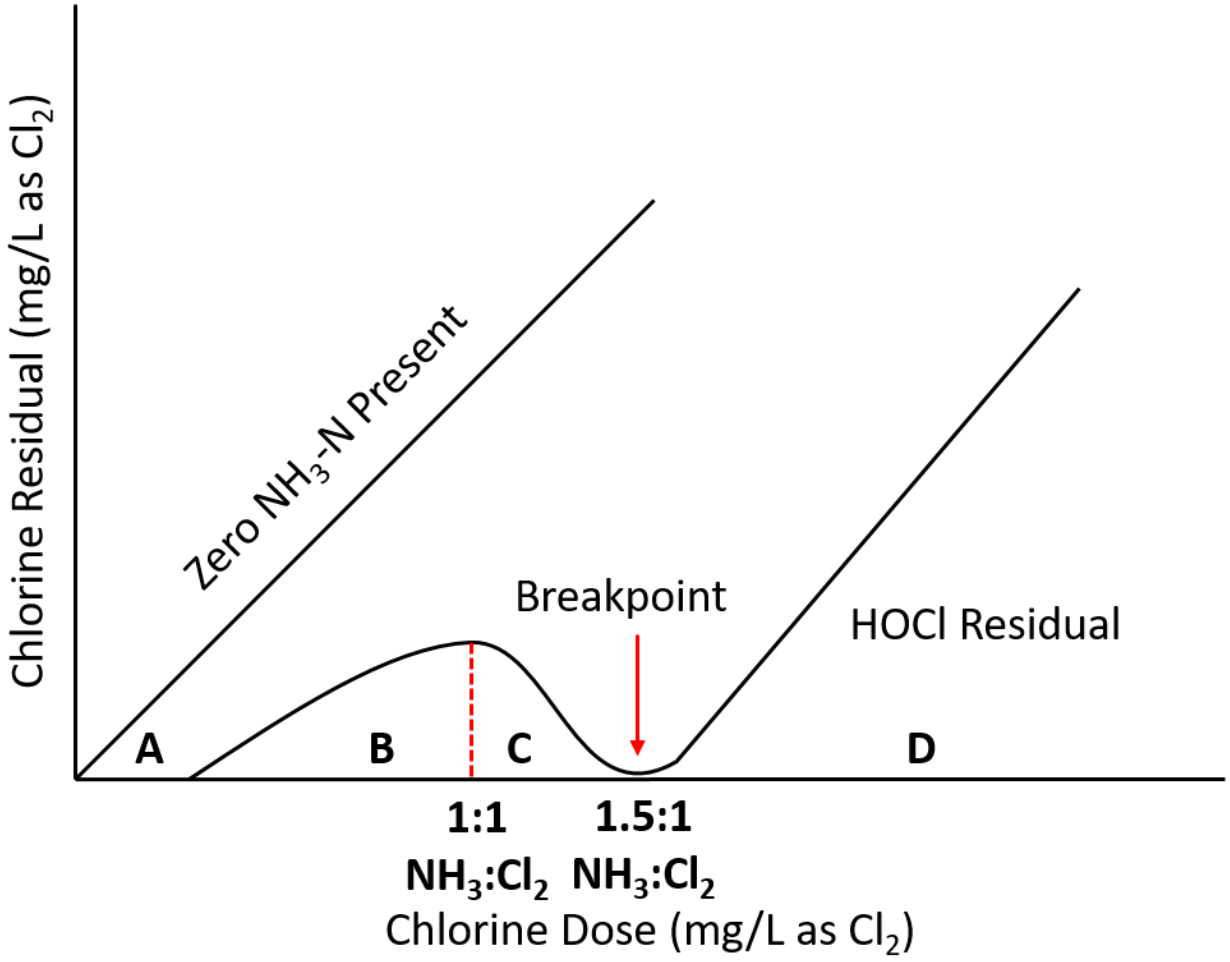

Figure 1-4: Breakpoint chlorination curve. **A**) Denotes the region where no residual is detected due to oxidation of reduced inorganic compounds. **B**) Only NH_2Cl forms until a molar ratio of 1:1 is reached. **C**) This area is denoted by the formation of NH_2Cl and $NHCl_2$. **D**) This area represents the residual once all nitrogenous and inorganic species have been oxidized, resulting in a free chlorine residual.

In a water matrix that has zero chlorine demand, the relationship between chlorine dose and chlorine residual is linear as denoted by the straight line in Figure 1-4. However, when ammonia is present in a water matrix, the relationship between chlorine residual and chlorine dose is no longer linear. [3] When ammonia and inorganic compounds are

present, the relationship changes. In Figure 1-4, the area denoted by “A” represents the lack of chlorine residual present due to oxidation of reduced inorganic species such as Mn(II), Fe(II), and NO_2^-. [3] Once all inorganics are oxidized, monochloramine will form up to a ratio of about 1:1 NH_3:Cl_2, as denoted by the dashed line and “B” in Figure 1-4 and Equation 1-1 (assuming only ammonia is present). [3] However, with increasing amount of chlorine, monochloramine will react with HOCl to produce dichloramine and trichloramine until the residual concentration approaches 0 mg/L or “breakpoint” as denoted by the red arrow in Figure 1-4 and Eq 1-4. [3] Breakpoint chlorination is typically achieved at a NH_3:Cl_2 ratio of 1.5:1. Once breakpoint chlorination is achieved, all dissolved ammonia is oxidized to nitrate and nitrogen gas as denoted by Equation 1-4. After breakpoint, a linear relationship between chlorine dose and chlorine residual is established as seen in Figure 1-4D.

Chloramines are less reactive and thereby more stable as residual disinfectants, however, they are known to produce N-DBPs. Unregulated N-DBPs are of concern because they have shown to be more toxic in Chinese hamster ovary (CHO) cells compared to regulated DBPs. [8, 19] For example, n-nitrosodimethylamine (NDMA) was identified as a chloramine DBP and is a powerful carcinogen with a 10^{-6} cancer risk level at a concentration of 7 ng/L. [2, 14, 20]

Ozone is another disinfectant more commonly used in Europe. [2] While ozone is an alternative disinfectant that produces lower levels of THMs and HAAs, high operating and capital costs makes it less feasible than chlorination. [17] Ozone reacts with organic matter to produce non-halogenated aldehydes, ketones, and carboxylic acids. [2, 17, 18] . Ozone oxidizes Br^- to form HOBr, as an intermediate species as shown in equation 1-5. HOBr

can further react with organic matter to produce brominated DBPs. [2, 18] Ozone can further oxidize dissolved halides (I^-, Cl^-, and Br^-) to iodate, chlorate and bromate.[2] Bromate (BrO_3^-) is classified as a "probable human carcinogen" by the U.S. Environmental Protection Agency (EPA) with a 10^{-6} cancer risk level at 50 ng/L. The maximum contaminant level in Canada for bromate is 10 µg/L

$$O_{3(aq)} + Br^-_{(aq)} + H^+_{(aq)} \rightarrow HOBr_{(aq)} + O_{2(aq)}$$

Equation 1-5[18]

Chlorine dioxide is used as a pre-disinfectant during the water treatment process. ClO_2 is more reactive than HOCl and is often produced on-site due to the dangers in transporting this chemical. [18] Unlike HOCl and NH_2Cl, ClO_2 does not react in substitution reactions with NOM and will not form significant organic DBPs. [2, 17, 18] However, ClO_2 degrades to chlorite (ClO_2^-) via a one electron transfer in the presence of an electron donor. [18] Chlorite has shown to possess cancerous properties. Yokose et al, observed that mice exposed to high doses of sodium chlorite developed lung adenomas, a benign lung tumor. [21] Chlorite has a MCL value of 1.0 mg/L in drinking water.

1.4 Gas Chromatography – Triple Quadrupole Mass Spectrometry

Chromatography is an analytical technique that separates chemical compounds (or analytes) within a matrix containing a chemical mixture. Figure 1-5 represents a general schematic on how gas chromatography (GC) works. Initially, the sample mix is injected into an inlet with a stream of ultra pure helium gas that carries the mix into the separation column. In the inlet, temperature ramps can be applied in order to help

volatilize the DBP mix in parts. This carrier gas is known as the mobile phase. [22] As the analyte mix is carried through the separation column, the analytes separate from the intermolecular interactions between the analyte and the coated capillary tubing, or stationary phase. The stationary phase is typically a polar or non-polar polymer. The retention of analytes on the column is dependent on their relative affinity to the stationary phase as well as the temperature settings of the oven. By adding a temperature gradient, the relative speed of the separation can increase as the analytes with less affinity to the column can move to the detector as shown in Figure 1-5. [22]

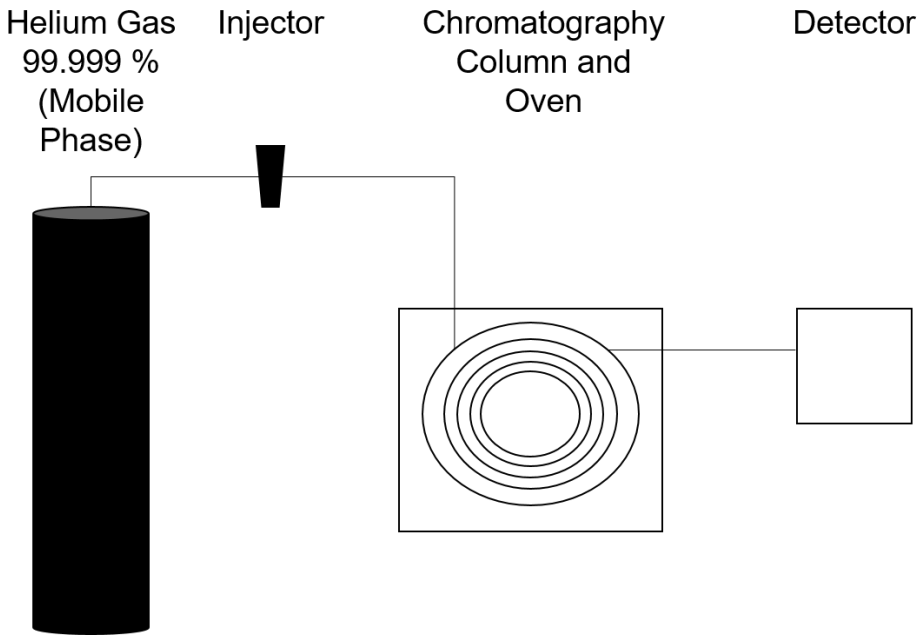

Figure 1-5: General schematic of gas chromatography system

Figure 1-6 shows what occurs in a capillary column. Contrary to liquid chromatography, the mobile phase of GC does not contribute to the speciation of analytes. [23, 24] In GC, selectivity and -retention of the analyte mixture is heavily influenced on the stationary phase. In this work, a polar capillary column was used (Restek RTX-200) as it offered acceptable separation for the 25 DBPs of all compounds with varying

polarity. The RTX-200 column is a triflouropropylmethyl polysiloxane stationary phase with mid polarity. In a previous method, a GC – time of flight (TOF) – mass spectrometer (MS) demonstrated narrow symmetrical peaks for the iodo – trihalomethanes (I-THMs). [25] This proves advantageous as the method in this work aims to characterize high priority DBPs of varying polarity where baseline resolved peaks prove beneficial.

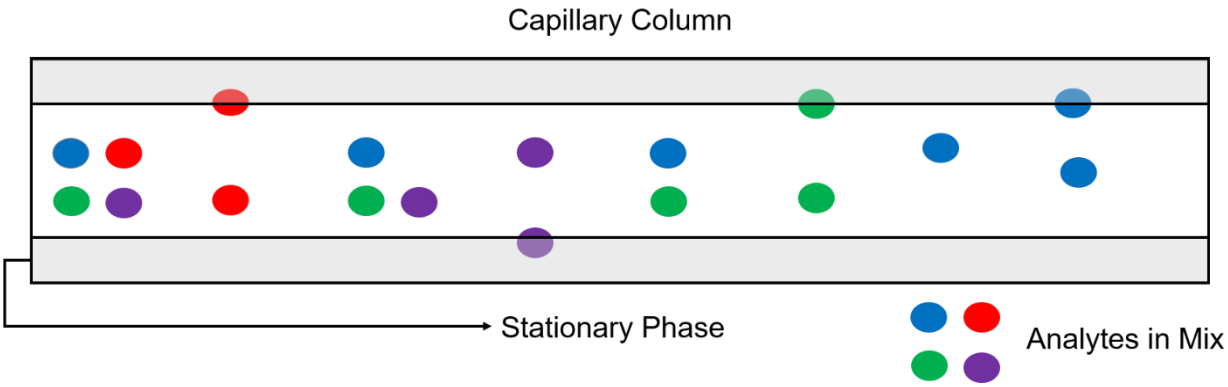

Figure 1-6: General schematic of capillary tube

After separation, analytes are transferred to a mass spectrometer for ionization and detection. Mass spectrometry (MS), or tandem mass spectrometry (MS/MS) is used for the structural characterization of compounds including organic, organometallic and biochemical compounds. There are multiple MS configurations, however, in this work we focused on tandem mass spectrometry.

MS/MS systems couple multiple mass analyzers in tandem that allow for a more sensitive and unambiguous form of detection compared to a MS system. The MS/MS system selects a precursor ion which is then collided with a neutral gas to produce fragments that are specific to the structure of the analyte. These fragments are used for quantitation and confirmation of the detected compound in a real sample. [26, 27]

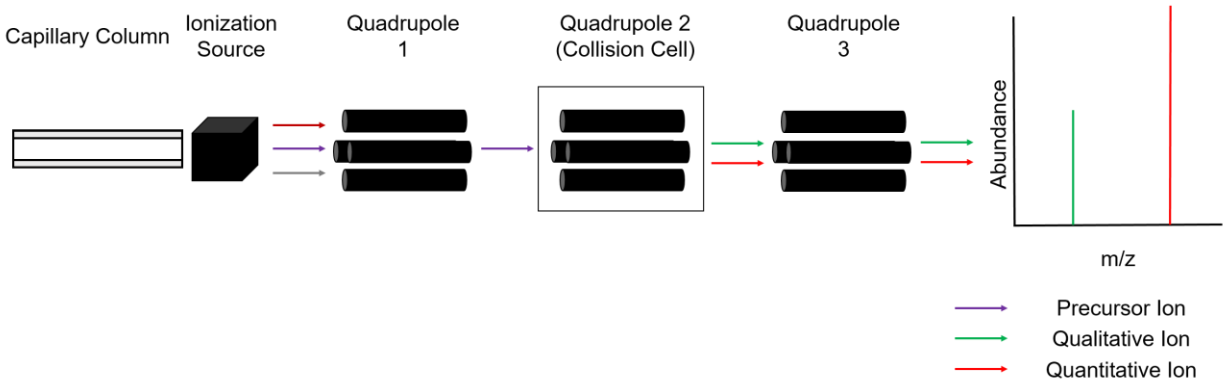

Figure 1-7: General schematic of a MS/MS system

A schematic of a MS/MS system is shown in Figure 1-7. First, separated analytes exiting the GC capillary column are bombarded with electrons to produce a charged fragment, a process known as electron ionization (EI). Typically, this ionization technique is considered “hard” because EI can destroy the molecular ion to produce several mass to charge (m/z) fragments. A molecular ion is known as the ion that is formed from the loss of one electron but is otherwise structurally intact. [26-28] Fragments produced by EI can be further speciated in the subsequent quadrupoles. The first quadrupole (Q1) selects the precursor ion by setting a specific radio frequency (RF) and direct current (DC) which allows only the precursor ion to pass into the collision cell (denoted by the purple arrow in the figure). [27, 29, 30] In the collision cell, the precursor ion is collided with gaseous nitrogen and a specific collision energy (CE) to produce fragments known as “product ions”. [27, 29, 30] The third quadrupole (Q3) can then scan or select specific product ions.

There are several advantages with a MS/MS system. The specificity that arises from two fragmentations results in a low noise to charge ratio that increases the sensitivity of the instrument. The compounds quantified in this study are small molecules that have similar structure. Therefore, this analytical method helps reduce interferences that can arise from analyzing compounds that share many structural and fragmentation patterns.

1.5 Analytical Methods for Disinfection By-product Analysis

Although there are several analytical methods for individual classes of DBPs, there are few studies that evaluate multiple classes of DBPs with GC-MS/MS. Table 1-4 contains DBP methods that analyze DBPs with GC-MS/MS for different water matrices.

Table 1-2: Published DBP Quantification Methods with GC – MS/MS

DBP Classes	LODs µg/L	Water Matrix	Extraction Method	Reference
7 HANs, 3 HNMs, 3 HALDs, 6 HKTs, 6 I-THMs	0.002 - 0.069	Secondary Effluent, UF/Effluent, UF/O_3, UF/RO	LLE	**This study**
11 HAAs	0.01 - 0.50	River Water	Derivatization -SPE	Kinani *et. al.* [31]
6 HAAs, 4 IAAs	0.025 - 0.10	Drinking Water	Derivatization-LLE	Cuthbertson *et. al.* [32]
6 HANs, 4 THMs, 2 HKTs, 1 HNM	0.003 - 0.014	Surface Water, Ground Water, Secondary Effluent	LLE	Liu, Y *et. al.* [33]
4THMs, 4 I-THMs, 6 HKTs, 1 HALD, 7 HANs, 4 HNMs	0.003 - 3.0	Tap Water, River Water	SPE	Roumiguières *et. al.*[34]

Kinani et. al focused on the quantification of eleven HAAs present in untreated river water samples. [31] Of these eleven HAAs, five of them were the regulated HAAs[31]. Overall, the aim of this work was to develop a fast and sensitive method on a GC – MS/MS in multiple reaction monitoring (MRM) mode, coupled with solid phase extraction (SPE), and chemical derivatization. They analyzed the performance of six SPE cartridges and compared percent recoveries of all eleven HAAs. After optimizing the extraction and choosing the Bakerbond SDB SPE cartridge, Kinani et. al. report percent recoveries between 42 – 100%, with an RSD between 7-13%. Samples also had to undergo derivatization in order to become amenable to GC – MS/MS analysis prior to extraction. Specifically, all HAAs underwent esterification for 2 hours at 50°C. This step adds a significant amount of time to sample prep, although Kinani et. al. argued that the SPE

procedure supposedly saves time when compared to a traditional liquid-liquid extraction (LLE) procedure. Lastly, the developed method reports limits of detections (LODs) ranging between 0.01 – 0.50 µg/L.

One of the disadvantages to this work is based on the limited analysis of DBPs. Kinani et al's work only focuses on one DBP class of which almost half of the analytes are regulated and have established methods of analysis. While this method might have lower detection limits than established methods, it does not prove beneficial for unregulated DBP analysis. Moreover, this method is only validated for river water, therefore validation studies would be needed in order to employ for wastewater effluents.

Cuthbertson et al. analyzed finished drinking water samples for a total of 61 DBPs using 3 analytical methods. However, only ten DBPs including 6 HAAs and 4 Iodo – Acetic Acids (IAAs) were analyzed with GC-MS/MS. DBP extraction employed LLE. The water samples were extracted with a 100 mL aliquot, 5 mL of MTBE, and 30 g of sodium sulfate (Na_2SO_4). Once all the reagents were combined the sample was shaken for a total of 3 x 15 mins, rested for 3 x 10 min, and used 5 mL x 3 of MTBE. Once concentrated, the samples were then derivatized using diazomethane to make the DBPs amenable to GC – MS/MS analysis. Percent recoveries in ultra – pure water (18MΩ) ranged from 27 – 33% for IAAs and 17 – 51% for HAAs. Limits of quantification ranged between 0.025 – 0.050 µg/L for IAAs and 0.100 µg/L for all HAAs. [32]

Cuthbertson et al's work has similar limitations, where only two classes of DBPs are studied with GC-MS/MS and required two additional analytical methods to evaluate multiple DBP classes. Also, the extraction method requires 10x the amount of sample volume (100 mL) than the work presented in this thesis (10 mL). The need for greater

amounts of sample results in longer extraction times which can prove tedious if many samples need to be ran simultaneously.

Liu et al. developed a method for a more comprehensive suite of DBPs for GC – MS/MS analysis including 6 haloacetonitriles (HANs), 4 THMs, 2 haloketones (HKTs), and 1 halonitromethane (HNM). Water samples included surface, ground, and wastewater at different locations in China. 30 mL of sample were extracted with 1.5 mL of MTBE and 12 g of Na_2SO_4 in a 40 mL amber vial. Percent recoveries reported for surface water, ground water and secondary effluent were 74.7 – 115.4 %, 86.1 – 120.6%, and 81.6 – 126.1%, respectively. The LODs reported for this method were between 0.003 – 0.014 µg/L. This was the only published study that evaluates DBPs in wastewater effluents with GC-MS/MS. While Liu et al's work used GC-MS/MS, it is limited to only 13 DBPs.

Roumiguiès et al. used GC – MS/MS instrumentation to analyze 4THMs, 4 I-THMs, 6 HKTs, 1 haloacetaldehyde (HALD), 7 HANs, and 4 HNMs. Water was taken from 18 river water and 4 tap water samples. The extraction method was SPE, however, this study optimized using the SPE Bakerbond SDB cartridge where several SPE cartridges were employed to evaluate which SPE cartridge resulted in larger recoveries, similar to Kinani et. al. [31] This work resulted in LODs between 0.003 – 3.0 µg/L. [34] Although Roumiguières et al. evaluated a more extensive list of DBPs, it was only validated for tap water and river water, and was not validated for wastewater effluents.

Overall, current DBP methods provide low level quantification that can quantify DBPs in drinking and surface water. However, our work aims to further increase the repertoire of unregulated DBP analysis by providing low method detection limits and

specifically, a method that is fully developed and validated for wastewater effluents. Furthermore, the work in this thesis also expanded the ability to detect a larger amount of DBP classes in one simultaneous run. Of all the methods listed in Table 1-4, only Liu et. al.'s work validated the method for secondary effluent. This method proves advantageous for closing some of the knowledge gaps of DBPs in wastewater effluents.

1.6 Motivation

The increase of the human population, global warming, and increasing anthropogenic compounds to waterways is compromising pristine water sources used for drinking water. Many developed countries have begun using wastewater as an alternative water source for potable reuse such as Singapore and the USA. However, it is not well understood what DBPs may form disinfection of wastewater-impacted waters. This study aims to 1) develop and validate an analytical method that can quantify 25 DBPs from 5 high priority DBP classes, and 2) evaluate the DBP formation potential from chlorination and chloramination in a full-scale wastewater reuse facility.

Chapter 2 describes the analytical method development for the quantification of 25 DBPs in wastewater samples using the GC-MS/MS. The development of the method involved running pure DBP standards to determine the quantifying (Q), qualifying (q) transitions, collision energies (CE), dwell times, and time segments. Then, parameters for LLE were improved in ultrapure water and methyl tert-butyl ether (MTBE) and validated in wastewater effluents. Percent recoveries from wastewater effluents were obtained by quantifying DBPs before and after standards spikes.

DBPs were evaluated in disinfected wastewater effluents and recycled waters in a full-scale wastewater reuse facility and described in Chapter 3. Samples were obtained

across the process treatment train to evaluate the removal of DBP precursors from four wastewater effluents. The sampled waters included in this study were secondary wastewater effluent, microfiltration (UF), UF/O_3, and UF/Reverse Osmosis (RO). Collected waters were disinfected under uniform formation conditions (UFC) using HOCl and NH_2Cl. UFC formation potential tests were chosen because the DBPs formed are representative of by-product formation in a real water treatment plant. Furthermore, sampling of these waters took place in Summer 2019, Fall 2019, and Winter 2020 to provide insight on how seasons affect the composition of effluent organic matter (EfOM) and therefore its impact on DBP speciation. Parts of Chapter 2 and 3 were taken from a submitted manuscript titled "Emerging disinfection by-product quantification method for wastewater reuse: trace level assessment using tandem mass spectrometry" to the journal Environmental Science: Water Research & Technology.

Chapter 2: Analytical Method Development for the Quantification of 25 DBPs in Wastewater using Gas Chromatography-Tandem Mass Spectrometry

2.1 Introduction

Water disinfection is used in drinking water and wastewater treatment to effectively control microbial pathogens that lead to waterborne diseases. However, organic matter and inorganic compounds (i.e. Br^-, I^-) that naturally occur in rivers and lakes can also react with disinfectants to produce disinfection by-products (DBPs). DBPs are always present in disinfected waters typically at µg/L levels. [6, 35] Although DBPs protect against immediate acute risks produced by microbial pathogens, they may also lead to potential chronic health problems caused by long-term exposure including bladder cancer and adverse birth outcomes. [36-46] Currently, guidelines and regulations have been established globally for 12 DBPs including THMs and HAA. [16, 35] However, more than 600 DBPs have been identified in surface or groundwaters disinfected with chlorine, chloramines, ozone, and chlorine dioxide. [35] Other DBP chemical classes include HANs, HNMs, HALDs, and HKTs.

The chemical and biological composition of source waters used for drinking water purposes are constantly changing as the result of population growth, climate change, and water scarcity. [47] Anthropogenic compounds (i.e, pharmaceuticals, personal care products, industrial chemicals) that are not well removed from treated wastewater are increasingly being found in lakes and rivers. [48, 49] Disinfectants also react with anthropogenic compounds which can potentially produce a different suite of DBPs compared to pristine waters. [50, 51] However, only a few studies have characterized the formation of unregulated priority DBPs (i.e., HANs, HNMs, HALDs, and HKTs.) in wastewater-impacted source waters and wastewater reuse. [52-60] Although recent

toxicological studies suggest that disinfected wastewater-impacted waters are more toxic than pristine waters, advanced water treatment including reverse osmosis and advanced oxidation processes may reduce the overall toxicity. [61, 62] It is critical to understand the efficiency of advanced and conventional treatment processes to remove or transform anthropogenic contaminants in source waters and bridging that knowledge gap to water toxicity.

Quantification of all DBP chemical classes could be laborious and intensive because most analytical methods are optimized for specific chemical and physical properties of a single DBP chemical class. [35, 63-66] Multianalyte methods that combine distinct chemical classes of unregulated DBPs have been developed in recent years which facilitates comprehensive DBP analysis. [25, 31-34, 67-70] However, these methods are mostly used for drinking water matrices and very few have been validated for wastewater impacted water sources. [33] Furthermore, as more studies evaluate the formation of unregulated DBPs from disinfection of pharmaceuticals, personal care products, and other environmental pollutants present in wastewater at parts per trillion levels.[63-66, 71] DBP analytical methods with higher sensitivity are needed.

The objective of this study was to develop a highly sensitive analytical method that can quantify DBPs in wastewater-impacted waters at parts per trillion levels. To achieve this, we employed a gas chromatography tandem mass spectrometry technology that reduce background ions and targets specifically for selected ions resulting in lower detection limits. Tandem mass spectrometry is advantageous because it can produce “precursor ions” from a target analyte, select a precursor ion and further fragment it to “product ions”. Quantification is based on selected product ions that have high signal to

noise ratio that leads to a highly sensitive method with almost no ambiguity. This highly sensitive quantification is advantageous for analysis of complex matrices such as secondary wastewater effluent where many contaminants and interferences exist in solution.

2.2 Material and Methods

2.2.1 Reagents and Solutions

DBP analytical reference materials listed in Table 1 were obtained at the highest purity available from Sigma Aldrich (St. Louis, MO), Toronto Research Chemicals (Toronto, ON, Canada), AccuStandard (New Haven, CT, USA), and Cansyn Chem. Corp. (Toronto, ON, Canada). Anhydrous acetonitrile and methyl *tert*-butyl ether (MTBE) were purchased from Acros Organics (New Jersey, NJ, USA). Ultrapure water (≥18.1 MΩ) was obtained from a Barnstead MicroPure system (Thermo Fisher Scientific, USA).

Individual reference standards were weighted and diluted in anhydrous acetonitrile to make ~4,000 mg/L stock solutions. Five 100 mg/L stock solutions for each DBP chemical class were prepared by mixing individual components in anhydrous acetonitrile. DBP chemical classes included haloacetonitriles (HANs), haloketones (HKTs), haloaldehydes (HALDs), halonitromethanes (HANs), and iodo–trihalomethanes (I-THMs). For example, a 100 mg/L stock mix of HALDs contained a mixture of dibromochloroacetaldehyde, bromodichloroacetaldehyde, and tribromoacetaldehyde. Individual and DBP mix stock solutions were stable for a year. Two master stocks were prepared daily prior to use by combining each DBP class to make 100 and 5 µg/L solutions. Master stocks were used to prepare neat standards and to spike ultra pure water samples.

2.2.2 Instrumentation

A gas chromatograph tandem mass spectrometer (GC-MS/MS) was used to quantify DBPs. The GC was an Agilent 7890B with multi-mode inlet (MMI) coupled to a 7000C Agilent triple quadrupole (Agilent Technologies, Santa Clara, CA). This system's ionization source was electron ionization (EI). The GC column used in this study was a Restek 200-Rtx column (30m x 0.25mm ID x 0.25 µm df) containing an inert mid-polarity crossbond trifluoropropylmethyl polysiloxane stationary phase. Previous studies have shown the advantages of this mid-polarity column when analyzing several DBP chemical classes. [25, 32] The GC oven program started at 35°C and was held for 5 min, followed by a temperature ramp of 9 °C/min to 220°C. A second temperature ramp of 20 °C/min to 280°C was programmed with a final hold of 20 min for a total run time of 47.6 minutes. Samples were injected as a pulsed-splitless injection with an inlet temperature program. The initial inlet temperature was 35°C and increased to 170°C at a rate of 360°C/min, followed by a second ramp of 720°C/min to a final temperature of 250°C. The injection pulse pressure of 20 psi was held for 0.75 min followed by an immediate purge to split vent of 30 mL/min. The transfer line and ion source temperatures were 250°C and 200°C, respectively.

The ionic transitions in the mass spectrometer were optimized by running a full scan of each DBP to observe the ion fragmentation pattern in each mass spectra. Typically, the base peak off all analytes were selected for a product ion scan. Once the product ion with the highest signal was obtained, parameters including collision energies, dwell times and time segments were optimized. The mass spectrometer was programmed under multiple reaction monitoring (MRM) mode with optimized parameters. Pure standards and

sample extracts were analyzed using the Agilent Mass Hunter (version 8.0) software for quantitation.

2.2.3 Calibration and Method Detection Limits

Calibration curve and method detection limits (MDLs) were determined from solutions prepared with ultra pure water that were spiked with the master stocks that contained all DBPs. The calibration curve solutions were prepared daily with concentrations of 0.001, 0.005, 0.01, 0.025, 0.05, 0.10, 0.25, 0.50, 1, 5, 10, and 25 µg/L. The calibration curves were separated in two parts in order to ensure linearity across all points. For low level quantification, a calibration curve using points between 0.001 - 0.50 µg/L were used. Other compounds were quantified with the upper half calibration points with a calibration curve ranging from 0.50 - 25 µg/L. Each calibration curve had a coefficient of determination (R^2) greater than 0.99 and had a linear range of three orders of magnitude.

MDLs were determined by the standard deviation of n=7 replicates multiplied by the 99% confidence interval of a one-sided Student's t-test as detailed elsewhere. [25] Briefly, MDLs were calculated using the equation below. Where CL is the concentration of all replicates in µg/L, $t_{N\text{-}1,1\text{-}a=0.99}$ is the 99% confidence level of n-1 Student's t-value, and $SD_{PeakArea}$ and $AV_{PeakArea}$ are the averaged standard deviation and peak areas, respectively. MDLs are reported on Table 1.

$$MDL = t_{N-1,1-\alpha=0.99} CL \frac{SD_{PeakArea}}{AV_{PeakArea}}$$

2.3 Results and Discussion

2.3.1 MS/MS Optimization: Transitions

Individual DBP neat standards were first analyzed in full scan mode to identify DBP transitions and determine retention times. The precursor ions were selected based on the base peak (most abundant ion) for most DBPs. However, the precursor ion for 1,1-dichloropropanone (11DCP), 1,1,1-trichloropropanone (111TCP), 1-bromo-1,1-dichloropropanone (1B11DCP), dichloroiodomethane (DCIM), and bromochloroiodomethane (BCIM) were selected based on the second strongest fragment peak. For example, 11DCP, 111TCP, and 1B11DCP all shared a common m/z base peak of 43.1 representing the $[COCH_3]^+$ fragment. This fragment was not selected because upon further fragmentation, the m/z of the product ions would be less than 32. A similar issue was encountered for DCIM where the m/z base peak of $[Cl_2CH]^+$ 82.9 led to a weak product ion response. For this reason, the m/z molecular ion peak $[CHCl_2I]^+$ 209.9 was selected as the precursor ion. BCIM had a base peak of m/z 126.9 that corresponded to $[I]^+$ ion. The selection of the 126.9 m/z peak was not possible for further fragmentation, therefore the molecular ion $[CHBrClI]^+$ with m/z of 255.9 was selected as the precursor ion. After the precursor ion selection, a product scan was obtained to determine the fragmentation pattern and select the two most abundant m/z ions as the quantification (Q) and qualification (q) ion. Results are shown in Tables 2-1.

Table 2-1: Ion fragmentations of DBPs and their quantifying and qualifying transitions

DBP	Fragment	Precursor Ion (m/z)	Fragment	Q Ion (m/z)	Fragment	q Ion (m/z)
CAN	$[CH_2ClCN]^+$	75.0	$[CHCl]^+$	48.0	$[CH_2CN]^+$	40.1
BAN	$[CH_2BrCN]^+$	120.9	$[CH_2CN]^+$	40.1	$[CH_2CN]^+$	41.1
IAN	$[CH_2ICN]^+$	166.9	$[CH_2CN]^+$	40.1	$[CH_2CN]^+$	41.1
DCAN	$[CHClCN]^+$	73.9	$[CCl]^+$	47.0	$[CHCN]^+$	40.1
DBAN	$[CHBrCN]^+$	117.9	$[CBr]^+$	90.9	$[CHCN]^+$	40.1
BCAN	$[CHClCN]^+$	73.9	$[ClC]^+$	47.0	$[CHCN]^+$	40.1
TCAN	$[CCl_2CN]^+$	107.8	$[CClCN]^+$	72.9	$[CCl]^+$	47.0
DCNM	$[CHCl_2]^+$	82.9	$[CHCl]^+$	48.0	$[CCl]^+$	47.0
DBNM	$[CHBr_2]^+$	172.8	$[CHBr]^+$	91.9	$[CHBr]^+$	93.9
BCNM	$[CHBrCl]^+$	128.9	$[CHCl]^+$	48.0	$[CCl]^+$	47.0
BDCAld	$[CHCl_2]^+$	82.9	$[CCl]^+$	46.9	$[CHCl]^+$	48.0
DBCAld	$[CHBrCl]^+$	128.9	$[CHCl]^+$	48.0	$[ClC]^+$	47.0
TBAld	$[CHBr_2]^+$	172.8	$[CHBr]^+$	91.9	$[CHBr]^+$	93.9
11DCP	$[CHCl_2]^+$	82.9	$[CCl]^+$	47.0	$[CHCl]^+$	48.0
13DCP	$[CH_2ClCO]^+$	77.0	$[CH_2Cl]^+$	49.0	$[CHCl]^+$	48.0
111TCP	$[Cl_2CCOCH_3]^+$	124.9	$[CCl_2CH_3]^+$	97.0	$[CHCl_2]^+$	82.9
113TCP	$[CH_2ClCO]^+$	77.0	$[CH_2Cl]^+$	49.0	$[CCl]^+$	47.0
1B11DCP	$[Cl_2CCOCH_3]^+$	124.9	$[CCl_2CH_3]^+$	97.0	$[CH_3CO]^+$	43.1
1133TeCP	$[CHCl_2]^+$	82.9	$[CCl]^+$	47.0	$[CHCl]^+$	48.0
DCIM	$[CHICl_2]^+$	209.9	$[CHCl_2]^+$	82.9	$[CHCl_2]^+$	84.9
BCIM	$[CHIBrCl]^+$	255.9	$[CHBrCl]^+$	128.8	$[CHBrCl]^+$	130.8
DBIM	$[CHBr_2]^+$	172.8	$[CHBr]^+$	91.9	$[CHBr]^+$	93.9
CDIM	$[CHICl]^+$	174.9	$[CHCl]^+$	48.0	$[CCl]^+$	47.0
BDIM	$[CHIBr]^+$	218.8	$[CHBr]^+$	91.9	$[CHI]^+$	140.0
TIM	$[CHI_2]^+$	266.8	$[CHI]^+$	140.0	$[I]^+$	127.0
I.S.	$[CH_2BrCHCH_3]^+$	120.9	$[CH_2Br]^+$	92.9	$[H_4C_3]^+$	41.1

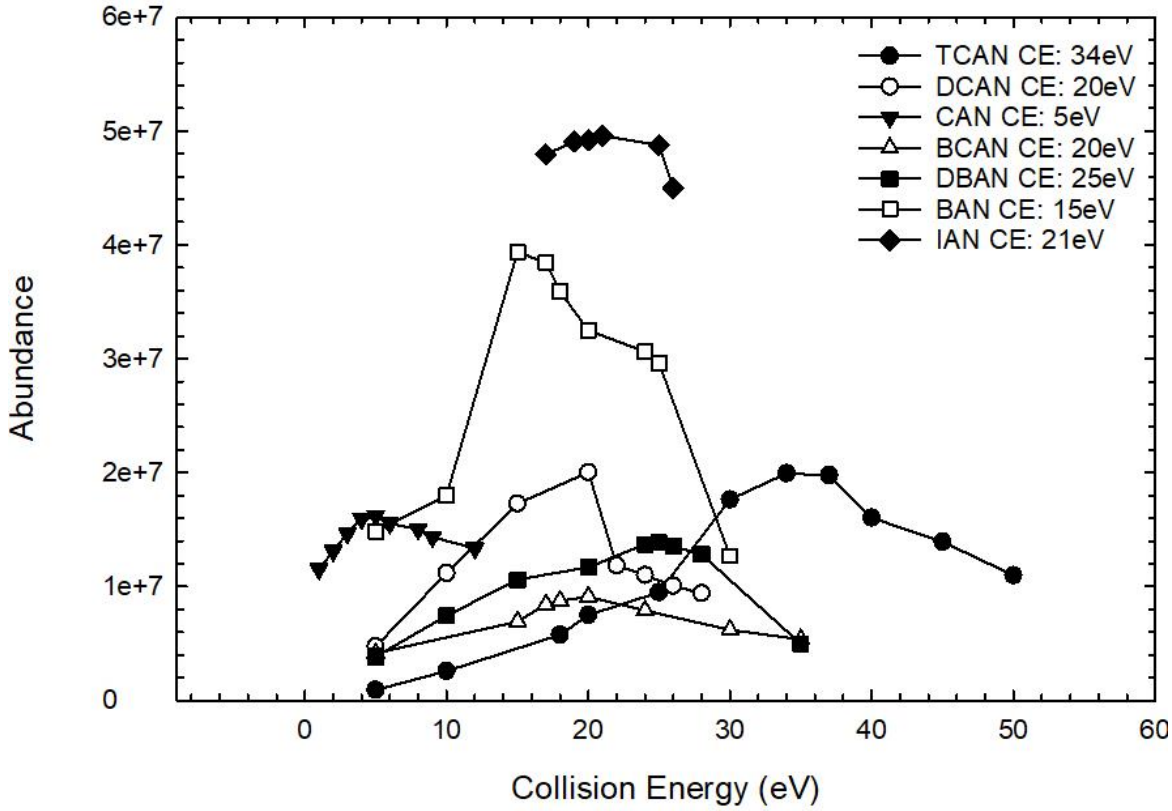

Figure 2-1: Collision energy (eV) optimization energies of the HAN class ranging from 0 – 50 eV.

2.3.2 MS/MS Optimization: Collision Energies

After DBP transitions were identified, collision energies (CE) were optimized to maximize the signal for each transition. First, HANs were optimized manually by incrementing the collision energy applied to each precursor ion. The CE was optimized once the maximum abundance was observed for the quantifier and qualifier transitions as shown in Figure 2-1. Manual optimization of CE values were compared to MassHunter's automatic "MRM transition optimizer" feature reported in Table 2-2. The automated CE values selected for the HANs class were in agreement with the manually optimized CE values, thereby validating the automated optimizer feature on Agilent's MassHunter. The MRM transition optimizer was then applied for the remaining DBPs. The

optimizer feature varied the CE with increments of 2 eV with range between 0 – 60eV. The software identified the CE that resulted in the highest abundance for each transition. All optimized CE are displayed in Table 2-2.

Table 2-2: Final parameters for all DBPs used in this method, including chemical transitions, dwell times, collision energies and recoveries in ultra – pure (18 MΩ Water).

DBP Class	DBP	Purity (%)	Abb.	Retention time (min)	MDLs (ng/L)	Percent Recovery[e]	Precursor (m/z)	Quantification Ion		Qualification Ion		Dwell Time (ms)
								m/z	CE (eV)	m/z	CE (eV)	
HAN	Chloroacetonitrile	99.5[b]	CAN	4.14	5.7	126.8	75	48	5	40.1	15	21.1
	Bromoacetonitrile	99.8[b]	BAN	6.69	3.6	120.8	120.9	40.1	10	41.1	10	18.3
	Iodoacetonitrile	98.1[b]	IAN	9.64	6.3	108.4	166.9	40.1	21	41.1	42	12.5
	Dichloroacetonitrile	99.4[d]	DCAN	3.86	3.2	91.4	73.9	47	21	40.1	32	22.2
	Dibromoacetonitrile	95.9[d]	DBAN	8.9	68.9	153.1	117.9	90.9	21	40.1	35	14.6
	Bromochloroacetonitrile	95.8[d]	BCAN	6.46	3.7	89.2	73.9	47	21	40.1	32	18.3
	Trichloroacetonitrile	98.0[d]	TCAN	2.95	3.2	34.1	107.8	72.9	29	47	60	21.7
HNM	Dichloronitromethane	96.2[a]	DCNM	4.85	4.1	109.2	82.9	48	52	47	55	27.8
	Dibromonitromethane	92.5[a]	DBNM	9.29	2.3	77.7	172.8	91.9	59	93.9	59	16.7
	Bromochloronitromethane	92.3[a]	BCNM	7.29	4.1	92.9	128.9	48	50	47	50	19.8
HAL	Bromodichloroacetaldehyde	94.2[a]	BDCAld	5.5	50.0	87.7	82.9	47	34	48	48	18.8
	Dibromochloroacetaldehyde	90.3[a]	DBCAld	7.91	11.9	106.6	128.9	48	48	47	50	18.8
	Tribromoacetaldehyde	97.3[b]	TBAld	9.94	13.0	111.7	172.8	91.9	59	93.9	58	20.8
HKT	1,1-dichloropropanone	95.5[d]	11DCP	4.69	25.7	108.5	82.9	47	43	48	43	23.3
	1,3-dichloropropanone	99.9[a]	13DCP	9.76	6.8	122.6	77	49	9	48	43	12.5
	1,1,1-trichloropropanone	98.7[d]	111TCP	7.64	30.6	62.9	124.9	97	9	82.9	9	18.8
	1,1,3-trichloropropanone	85.0[c]	113TCP	10.87	7.5	134.2	77	49	10	47	46	40.8
	1-bromo-1,1-dichloropropanone	96.0[c]	1B11DCP	9.68	56.2	84.7	124.9	97	2	43.1	22	20.8
	1,1,3,3-Tetrachloropropanone	92.7[a]	1133TeCP	11.74	5.5	138.2	82.9	47	43	48	34	33.3
I-THMs	Dichloroiodomethane	99.9[a]	DCIM	4.12	5.7	88.3	209.9	82.9	1	84.9	12	22.2
	Bromochloroiodomethane	99.0[a]	BCIM	6.4	7.5	72.1	255.9	128.8	2	130.8	11	15.4
	Dibromoiodomethane	93.9[a]	DBIM	8.52	2.0	69.9	172.8	91.9	57	93.9	57	18.8
	Chlorodiiodomethane	99.9[a]	CDIM	9.02	3.6	53.2	174.9	48	53	47	60	20.8
	Bromodiiodomethane	92.5[a]	BDIM	10.8	5.6	52.0	218.8	91.9	60	140	60	45.8
	Iodoform	99.0[b]	TIM	12.74	3.1	49.2	266.8	140	60	127	60	50.0
I.S.	1,2-dibromopropane	97.0[b]	I.S.	6.31	N/A	N/A	120.9	92.9	30	41.1	10	16.3

[a]CanSyn Chem Corp [b]Sigma Aldrich [c]Toronto Research Chemicals [d]AccuStandard [e]Percent recoveries are for final conditions detailed in Table 3
I.S.: internal standard; N/A: not applicable; MDLs: method detection limits; Abb.: abbreviation

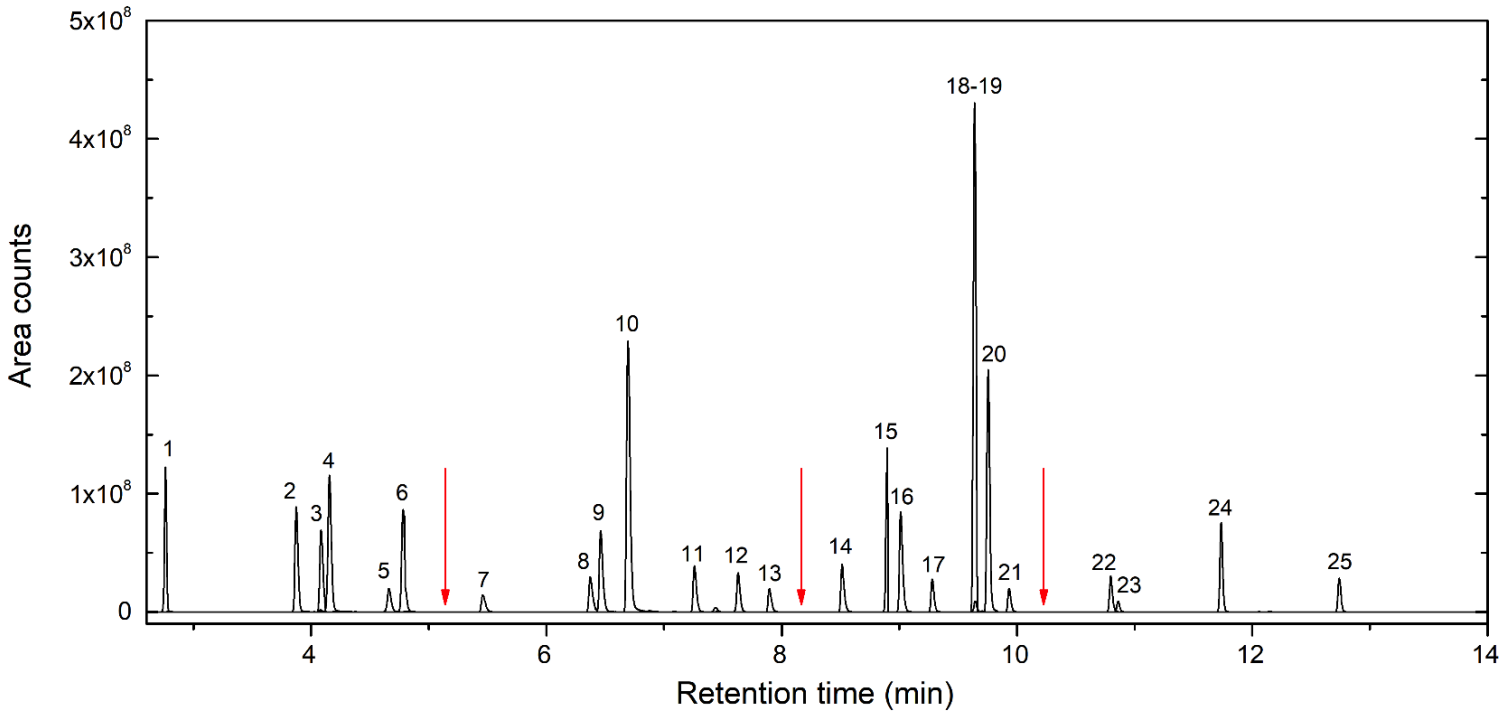

Figure 2-2: Chromatographic separation of 25 DBPs. Red arrows indicate time segments

2.3.3 MS/MS Optimization: Time Segments

In order to increase sensitivity of the instrument, time segments were introduced into the method. Time segments ensure higher sensitivity of the triple quadrupole by reducing the number of chemical transitions to scan for per segment. [72] A total of four time segments were included as shown in Figure 2-2: 0.00-5.20, 5.20-8.20, 8.20-10.20, and 10.20-47.60 minutes. Each time segment had 6, 7, 8, and 4 DBPs, respectively. Additionally, each segment was selected when target peaks were not present (Figure 2-2). The time gap between the peaks ensured that the quadrupoles and software had enough time to adjust for the scans included in the next segment.

2.3.4 MS/MS Optimization: Dwell Times

Another parameter that was optimized for this method was the dwell time for each analyte. Dwell time refers to the sampling or scanning time spent for each peak during the MRM. [73]Typically, longer dwell times result in a higher number of ion hits to the detector resulting in an increased sensitivity of the analyte. Peak shape is dependent on dwell times as seen in the equation below

$$Dwell\ time\ (ms) = \frac{pw}{tr * 15}$$

where, pw is the peak width in milliseconds, and tr is the number of total transitions in each time segment. Literature reports that 12-20 points per peak results in an acceptable peak shape that increases accurate quantitation and reproducibility of peak shape. [74, 75] In our study, 15 data points were used in the equation to determine appropriate dwell time. For example, in the first time segment there were six analytes with two transitions each which corresponded to a total of 12 transitions per segment. The range of dwell times is due to the number of transitions per time segment resulting with dwell times between 12.5-50.0 ms as observed in Table 2-2. Chromatographic separation of all analytes with optimized collision energy, segment time and dwell time are shown in Figure 2-2.

2.3.5 Liquid-Liquid Extraction: Sample Volume Reduction

DBPs are small volatile molecules that are extracted with LLE. [25, 32, 67-70] However, LLE is time consuming and is typically the limiting step for DBP analysis for most cases. Cuthbertson et al. LLE method was modified in this study, to reduce time and resources increasing analysis capacity. [32]Due to the increased sensitivity that comes with a MS/MS system, the sample extract concentration was reduced, thereby requiring less sample and solvent volume, salt, and overall analysis time. First, three sample volumes (100, 50 and 10 mL) were evaluated under similar conditions (Exp. 1, 2, and 4) as described in Table 2-3. Sodium sulfate was adjusted according to the sample volume to achieve salt saturation of 0.3 g/mL. LLE was performed three times for all experiments. Percent recoveries are plotted for all DBP classes in Figure 2-3 A-E.

Table 2-3. Recovery percentage of each DBP spiked at 100 ng L^{-1} for each Experiment 1-4.

Variable	Experiment 1	Experiment 2	Experiment 3	Experiment 4
Sample Volume (mL)	100	50	50	10
Organic Solvent (mL)	5 x 3	5 x 3	5 x 3	3 x 3
Sodium Sulfate (g)	30	15	15	3
Shake Time (min)	15	15	15	15
Rest Time (min)	15	15	15	15
Final Extract Volume (µL)	200	200	100	200

In general, percent recoveries were reduced by about half when sample volume was reduced from 100 (Exp. 1) to 50 mL (Exp. 2). However, Figure 2-3C depicts the HKT recoveries. Experiment 2 resulted in 0% recovery for all HKTs except 1B11DCP and 113TCP where recoveries were less than 10% for each HKT. The overall complete loss of recovery for most HKTs and approximately 50% loss for all other classes may be

attributed to the size of the amber bottle used. The sample size of 50 mL in Exp 2 required the use of a 125 mL amber bottle, resulting in almost 50% headspace once all other reagents were added. The aggressive shaking of the bottles, coupled with the headspace, may have resulted in volatilization of the DBPs, thereby resulting in decreased recoveries.

However, when sample volume was reduced to 10 mL (Exp. 4) similar percent recoveries were obtained compared to 100 mL sample volume. Similar results were also observed with HNMs and HALDs therefore, a sample volume of 10 mL was used for further optimization. Additionally, two final extract volumes, 200 and 100 µL, were also evaluated (Exp. 2 and 3). Percent recoveries obtained in Experiment 3 were slightly higher compared to Experiment 2 however, a final volume of 100 µL was found difficult to work with during the nitrogen blowdown that could lead to a higher error in the method. Therefore, a final extract volume of 200 µL was used.

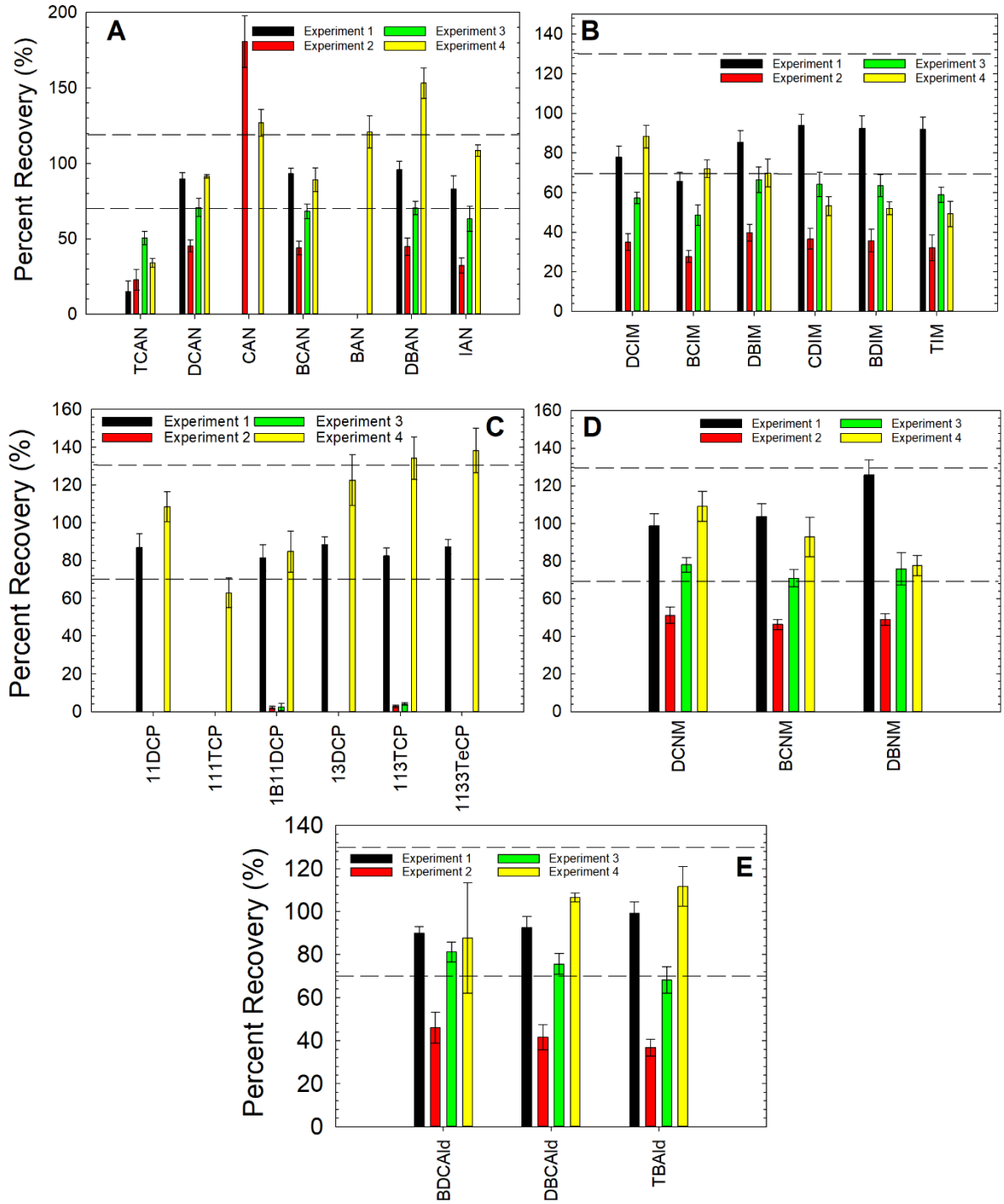

Figure 2-3: **A)** Extract and sample volume for HAN class reported as percent recoveries. **B)** Extract and sample volume for I-THM class reported as percent recoveries. **C)** Extract and sample volume for HKT class reported as percent recoveries **D)** Extract and sample

volume for HNM class reported as percent recoveries **E)** Extract and sample volume for HALD class reported as percent recoveries. Dashed lines represent acceptable percent recovery range between 70-130%.

2.3.6 Liquid-Liquid Extraction: Solvent Volume and Shake Time

Solvent volume (1, 3, and 5 mL) and shaking time (5, 10, 15 min) were also reduced. LLE was performed three times for each solvent volume. Percent recoveries are shown in Figure 2-4 A,B,C. Initial extraction conditions of 5 mL x 3 for 15 min (Figure 2-4 C) had the best analyte percent recoveries (> 70%) except for trichloroacetonitrile (TCAN). Similar results were observed with a lower solvent volume of 3 mL x 3 as shown in Figure 2-4 B. The majority of analytes had recoveries > 70% for a 10 and 15 min shake times. Although reducing solvent volume may adversely affect analyte extraction efficiency from water samples, it can also reduce time required to concentrate the extract thereby minimizing analyte loss due to volatilization. However, when 1 mL x 3 was evaluated percent recoveries were significantly lower than 70% (Figure 2-4 A). Therefore, solvent volume and shaking time was tested at 3 mL x 3 and 10 minutes, respectively. Final sample extraction conditions are summarized in Table 2-4 which reduced overall sample extraction time by half compared to initial conditions (Experiment 1).

Table 2-4: Sample extraction: initial and final conditions

Variable	Initial Conditions [32]	Final Conditions
Sample Volume	100	10
Organic Solvent	5 x 3	3 x 3
Sodium Sulfate (g)	30	3
Shake Time (min)	15	10
Rest Time (min)	15	5
Total extraction time (6 samples in duplicate)	4 hours	2 hours

[32](Cuthbertson et al., 2020) [b]this work

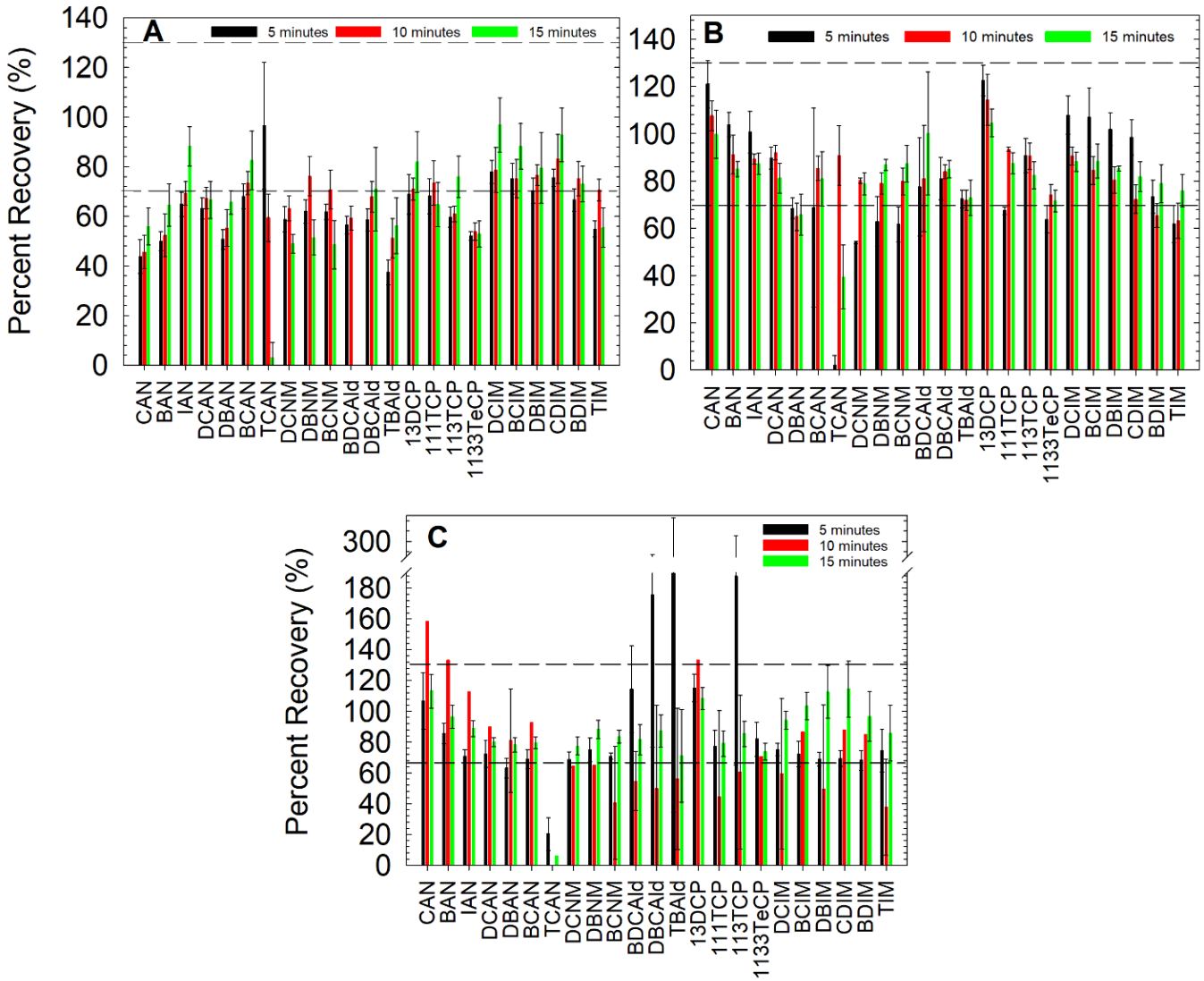

Figure 2-4: Testing of three shake times for 1 mL x 3 of MTBE solvent extraction **(A).** Testing of three shake times for 3 mL x 3 of MTBE solvent extraction **(B)**. Testing of three shake times for 5 mL x 3 of MTBE solvent extraction **(C)**. All recoveries were performed in triplicate and average recovery is plotted. Dashed lines represent the acceptable range for DBPs (70-130%).

2.3.7 Percent Recoveries and Matrix Effects

Analyte percent recoveries for 100 ng/L spikes for initial and final conditions (Table 2-4) are shown in Figure 2-5A. Initial percent recoveries determined in this study ranged between 31–142% which agrees with values obtained by Cuthbertson et al between 30-110%. [32] TCAN had the lowest recovery at 31.3% which is slightly higher than previously reported at 20%. TCAN low recovery might be linked to TCAN's lower boiling point (84°C) that indicates a higher volatility compared to other HANs that have boiling points ≥110°C. In the sample extraction process, solvent extracts are blown down under a slow nitrogen stream where TCAN could have been lost in the process. At final conditions, it was observed that percent recoveries for 16 DBPs remain about the same especially for I-THMs. Higher recoveries were also observed for chloroacetonitrile (CAN), bromoacetonitrile (BAN), and 1,3-dichloropropanone (13DCP). However, dibromoacetonitrile (DBAN), dichloronitromethane (DCNM), bromochloronitromethane

(BCNM), 1,1,3,3-tetrachloropropanone (1133TeCP), bromodichloroacetaldehyde (BDCALD), and dibromochloroacetaldehyde (DBCALD) had lower percent recoveries compared to initial conditions. The final conditions obtained percent recoveries within 70-130% except for DBAN, TCAN, 111TCP, 113TCP, 1133TeCP, iodoform (TIM), BDIM, DBIM and, CDIM. Furthermore, percent recoveries at a higher spike level of 5 µg/L at final conditions (Figure 2-5B – Ultra Pure Water) were between 31-104%.

Sample extraction from different matrices other than ultra pure water could affect the efficiency to recover analytes. Figure 2-5B illustrates the recovery of each analyte from ultra-pure water and secondary wastewater effluent. DBP percent recoveries from

secondary effluents (29-83%) for most analytes were slightly lower compared to ultrapure water extractions (31-104%). HNM percent recovery dropped from 84 - 104% in ultra pure water to 61-73% in wastewater effluents. However, calibration curves are obtained from known spiked waters that undergo the sample extraction process. For this reason, although absolute percent recoveries determined in Figure 2-5B are important, the main concern for the method's precision is the difference between both matrices. The difference between ultrapure and wastewater recoveries were between 0.5-30% which were found to be acceptable.

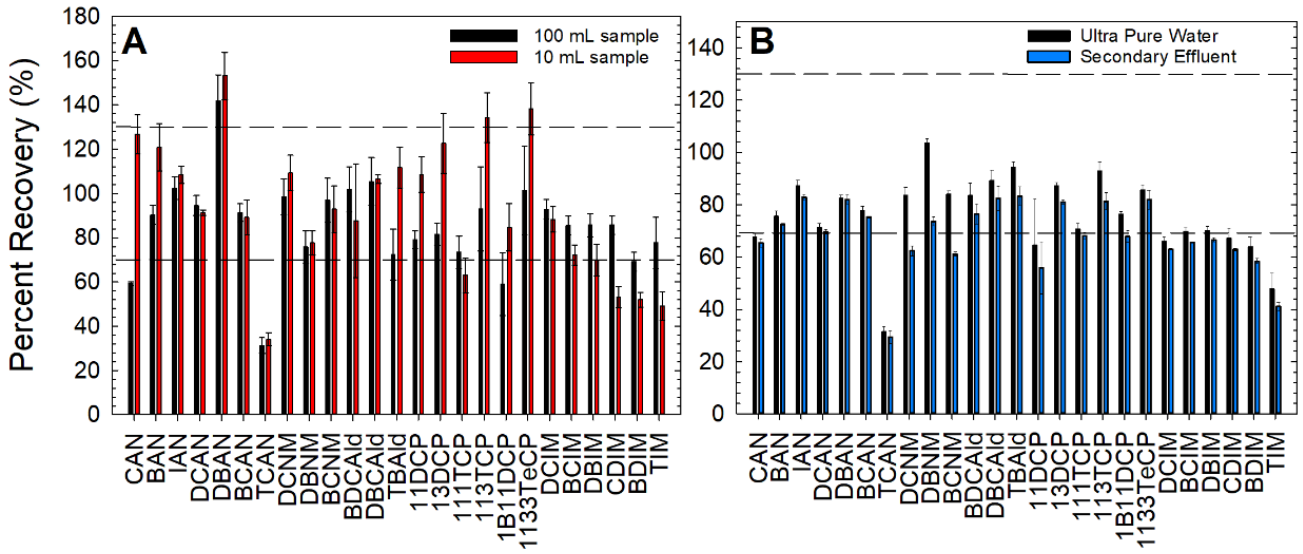

Figure 2-5: **(A)** Percent recoveries obtained from 100 ng/L spikes of analytical standards in ultra-pure water. Extractions were performed in triplicate and results are shown as an average. Dashed lines represent acceptable percent recovery range between 70-130%. **(B)** percent recoveries obtained from 5 µg/L spikes of analytical standards in ultra-pure water (black bars) and secondary effluent (blue bars). Extractions were performed in triplicate and results are shown as an average.

2.3.8 Method Validation and Reproducibility

A study was performed to observe the reproducibility and precision of the analytical method. An acceptable precision is acceptable when the RSD is about 10% of less. Precision of the instrument was also tested for all analytes at a low (100 ppt) and mid, (250 ppt) and high concentrations (100ppb). Replicate injections (n=7) of all analytes were injected from the same vial to test the precision of the instrument. Precision was calculated by displaying the %RSD for each analyte at each concentration listed below in Table 2-5. The majority of analytes displayed low RSD (<3.1%) with higher concentrated samples however, TCAN displayed high RSD with an average of 60% for all spikes.

Table 2-5: Precision RSD values of all compounds injected (n=7) at 100 ng/L, 250ng/L, and 100 µg/L.

	RSD (%)		
DBP	100 ng/L	250 ng/L	100 µg/L
CAN	5.7	4.6	2
BAN	7	3.8	1.1
IAN	8.2	7.9	0.9
DCAN	4.6	3.6	1.4
DBAN	10.1	10.7	1.6
BCAN	8.8	5.4	2.1
TCAN	43.9	98.8	36.0
DCNM	6.5	5.4	1.5
DBNM	9.1	7.1	2.9
BCNM	8.8	8	1.1
BDCAld	< MDL	22.6	3
DBCAld	9.6	5	1.3
TBAld	10.3	10	2.6
11DCP	< MDL	4.5	3.1
13DCP	8.6	6.5	1
111TCP	10.6	9.1	1.7
113TCP	10.4	9.1	0.8
1B11DCP	7.3	7.9	1.7
1133TeCP	11.4	10.5	1.6
DCIM	6.4	6.7	2.3
BCIM	6.8	13.6	1.8
DBIM	8.2	7.9	1.1
CDIM	6.7	9.5	1.2
BDIM	9.9	10.7	1.1
TIM	8.7	8.9	1.2

2.4 Conclusions

A novel GC-MS/MS method was developed and validated for the simultaneous quantification of 25 DBPs in treated wastewater effluents. In order to obtain low-level quantification, several parameters were optimized on the mass spectrometer including collision energy, dwell times, and time segments. Collision energies were optimized in order to produce a large m/z signal of the Q and q ion transitions for all DBPs. Moreover, dwell times were determined to ensure good peak shape (15 points per peak) and reproducibility at trace level quantification. Additionally, four time-segments were also implemented in the analytical method to increase sensitivity of the detector by limiting the transitions to scan for in each segment.

The sample extraction process was also improved to reduce the amount of sample volume. Initially, four experimental conditions were tested to reduce initial sample size and the final volume of the extract (Figure 2-3 A-E). Then, the shake time was also tested to reduce the overall extraction time and increase sample throughput (Figure 2-4 A-C). The final sample size was reduced from 100 mL to 10 mL with and overall extraction time reduced by half.

After the MS/MS optimization and sample extraction reduction, the method was validated in ultra pure and secondary effluent waters with recoveries between 31-104% and 29-83%, respectively. Overall, the method improvement lead to MDLs ranging from 2.0-68.9 ng/L for this GC-MS/MS method.

This method will be used to evaluate DBP formation potential in secondary effluent, UF, UF/Ozone, and UF/RO waters. Each sample will be collected at an advanced wastewater treatment plant and disinfected with chlorine and chloramines. Finally, all

samples will be quenched using ascorbic acid, extracted, and injected in to the GC-MS/MS.

Chapter 3: DBPs in a Full Scale Reuse Facility

3.1. Introduction

This work evaluates the efficacy of DBP precursor removal from secondary wastewater effluents with advanced treatment processes including microfiltration (UF), UF-ozonation (O_3), and UF – reverse osmosis (RO). DBP precursor removal is characterized by the amount of DBPs formed post-disinfection. Therefore, if less DBPs are formed after a treatment process, this can be regarded as an efficient treatment step. This analytical method quantifies 25 high priority DBPs. Information on DBP composition of treated wastewaters is necessary to assess the toxicological properties of finished wastewaters for potable reuse. [19, 58, 69]

This research is the first to comprehensively evaluate DBP formation potential of priority DBPs from chlorination and chloramination across a full-scale reuse facility in Canada. Mitch et al. conducted similar studies where halogenated DBPs were characterized from advanced potable reuse treatment trains in the United States. [55, 60] However, Mitch et al. characterized DBPs within the treatment train and only in disinfected RO effluents. The efficacy to remove DBP precursors from each process was not evaluated. In this study, DBP precursors removal was evaluated by conducting DBP formation potential at each individual treatment step.

The need to recycle wastewater for potable reuse may become the only option in some areas in the future as climate change and population growth continues to impact and deplete pristine freshwater sources available for consumption. This contributing factor further drives the need to characterize the DBP speciation in wastwater effluents.

3.2 Materials and Methods

3.2.1 Advancing Canadian Wastewater Assets (ACWA)

Wastewater effluents were collected from Advancing Canadian Wastewater Assets (ACWA), a full-scale research plant that treats secondary wastewater effluents with microfiltration (UF), followed by reverse osmosis (RO) or ozone treatment (O_3) as shown in Figure 3-1. The wastewater treatment process includes screen and grit removal, primary clarifier, activated sludge reactor, and secondary clarifier. Samples were collected in 1L HDPE bottles with no headspace and were stored at 4°C. Water quality parameters are shown in Table 3-1, below. Samples were extracted with improved conditions and analyzed for DBPs as controls prior to formation potential testing. Sampling events were conducted in summer, fall, and winter on days where the wastewater treatment plant was also sampling. This was done in order to obtain as many water parameters as possible. Water quality parameters are shown in Table 3-1.

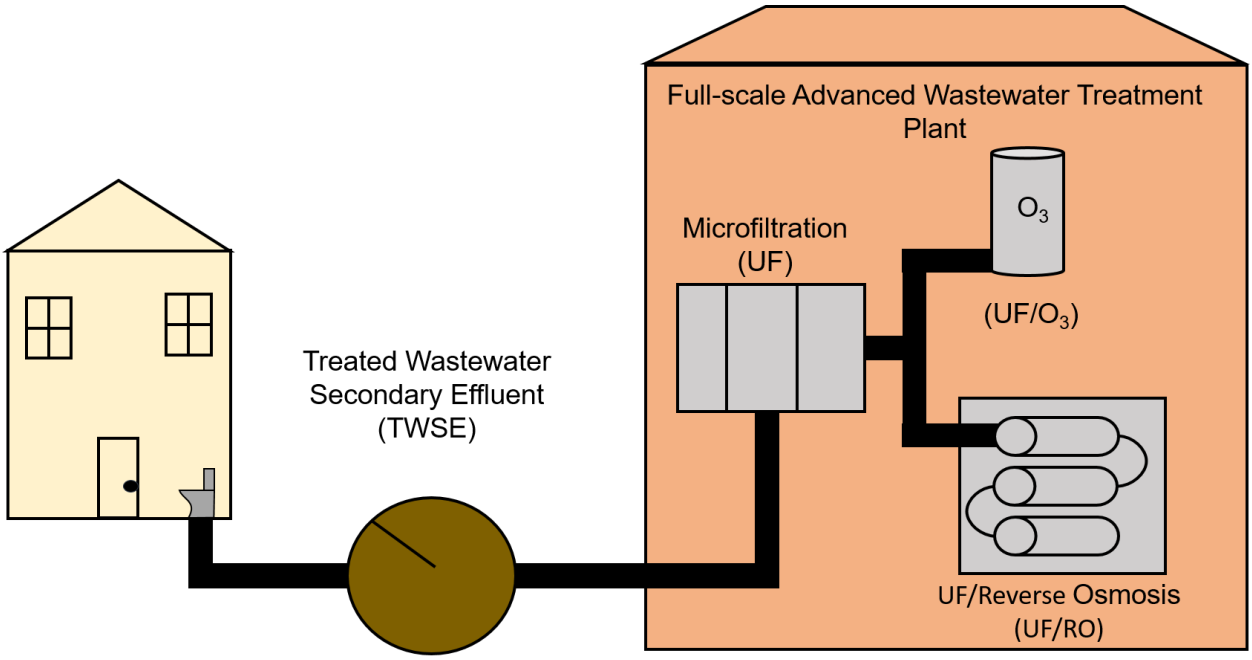

Figure 3-1: Sampling port location schematic

3.2.2 Water Samples & Formation Potential Testing

Formation potential testing was performed under uniform formation conditions (UFC) to compare DBP formation across four different water matrices. Chlorination (HOCl) and chloramination (NH_2Cl) of water samples were performed following the UFC protocol detailed elsewhere. [76] Briefly, water samples were filtered through 0.45 µM polyethersulfone membrane disc filters prior to disinfection. All reagents were prepared using ultra pure chlorine demand free water (CDFW) to prevent any consumption of disinfectant by reagents. Hypochlorite dosing solutions (3,000-10,000 mg/L as Cl_2) and chloramine (1,500 mg/L as Cl_2) were prepared daily as explained elsewhere. [77, 78] Filtered samples (400 mL) were spiked with 0.8 mL of 1M borate buffer and adjusted to an overall pH of 8.0 ± 0.2 using H_2SO_4/NaOH solutions. Dosed samples were transferred to 125 mL amber bottles without headspace and incubated for 24 ± 1 hr to achieve a chlorine residual between 0.60 – 1.40 mg/L as Cl_2. Chlorine residual and dosing solutions were quantified using a colorimetric standard method 4500-Cl. [79] All samples were quenched with 1.5:1.0 molar ratio of ascorbic acid to Cl_2 once the chlorine residual was measured (Table 3-1). Quenched samples were immediately extracted and quantified.

Table 3-1: Water quality parameters of all sampling events

Sampling Event	Matrix	DOC (mg/L as C)	TN (mg/L as N)	NH_3 (mg/L)	pH	Cl^- (mg/L)	Br^- (µg/L)	$SUVA_{254}$	Chlorine Residual (mg/L as Cl_2)	
									HOCl	NH_2Cl
Summer June 11, 2019	Secondary Wastewater Effluents	10.16	9.29	<0.04	7.9	N/A	N/A	N/A	1.39	1.65
	Microfiltration /Ozonation	7.69	7.99	0.06	7.7	N/A	N/A	N/A	1.25	0.93
	Microfiltration /Reverse Osmosis	< 0.2	0.44	0.04	6.3	N/A	N/A	N/A	0.95	1
Fall October 9, 2019	Secondary Wastewater Effluents	7.38	8.53	0.91	7.2	121	55.6	N/A	1.02	1.2
	Microfiltration	7.27	7.56	0.07	7.2	119	82.8	N/A	1.19	0.76
	Microfiltration /Ozonation	6.01	7.74	0.13	7.1	124	39.6	N/A	1.41	1.1
	Microfiltration /Reverse Osmosis	<1.00	0.35	<0.04	5.7	3.48	1.54	N/A	0.81	0.79
Winter February 6, 2020	Secondary Wastewater Effluents	7.37	10.39	<0.04	7.3	122	N/D	2.11	0.6	1.23
	Microfiltration	6.98	N/A	<0.04	7.2	151	N/D	2.11	0.69	1.04
	Microfiltration /Ozonation	7.30	8.55	0.04	7.0	116	N/D	0.9	<2.0	1.43
	Microfiltration /Reverse Osmosis	<0.20	0.49	<0.04	6.4	3.25	N/D	N/D	0.93	1.03

DOC: Dissolved organic carbon
TN: Total nitrogen
N/A: Not available
N/D: Not detected
Iodide was not detected in samples

3.2.3 DBP and TOX Analysis

Target and non-target DBP analysis were conducted for this study. The validated method described in Chapter 2 was used to analyze 25 target DBPs. Total organic halogen (TOX) was used for non-target DBP analysis. The TOX method was followed as outlined by Kimura et. al with the following modifications. [80] The furnace program for the activated carbon (AC) columns was changed to 500 seconds at the end position, 200 seconds at the cooling position, and 200 seconds at the home position with argon and

oxygen flow rate of 200 and 400 mL/min. A 0.02 mM ammonium buffer was used as the absorption solution to collect the furnace off-gases. The absorption solution was analyzed for chloride, bromide, and iodide using a Dionex Integrion Ion Chromatograph (Thermo Fisher Scientific, USA) and a 2mm Dionex ADRS 600, anion dynamically regenerated suppressor was used. The chromatographic column used was a Dionex IonPac AS20 Analytical Microbore Column (250 mm x 2mm ID). The method detection limits for total organic chlorine (TOCl), total organic bromine (TOBr), and total organic iodine (TOI) are 0.5 µg/L, 1.0 µg/L, and 1.0 µg/L, respectively.

3.3 Results and Discussion

3.3.1 Summer 2019: DBPs in Advanced Treatment of Secondary Wastewater Effluents

All samples collected in Summer 2019 were from secondary wastewater effluents, secondary effluent treated with microfiltration membranes and ozonation (UF/O_3), and three reverse osmosis membranes (UF/RO). It should be noted that UF effluents were not sampled during the first sampling event which is why only three effluents are present instead of four. Three DBPs were quantified in total, including DCAN, BCAN, and 11DCP as shown in Figure 3-2B. DCAN, and 11DCP were quantified in secondary effluent at 23 ng/L and 85 ng/L, respectively.

Both of these DBPs experienced an increase in concentration upon subsequent UF and O_3 treatment (Figure 3-2 A, B) leading to 100 ng/L and 142 ng/L concentration for DCAN and 11DCP, respectively. This increase in concentration has been observed previously where haloacetonitriles and haloketones have been identified as ozonation by-

products as reported by Richardson et al. [35] Furthermore, BCAN was also detected in UF/O_3 effluents at 8 ng/L. The formation of brominated DBPs in ozonated waters is well known due to ozone's ability to readily oxidize bromide to HOBr, which subsequently reacts with organic matter to form brominated DBPs. [18]

Lastly, UF/RO waters reduced DCAN concentration by 76% from secondary effluents to finished RO waters. DCAN was quantified at 5 ng/L after RO. Similar results were observed in a previous study demonstrating poor RO-rejection of DCAN, consistent with the results observed in this study. [81]

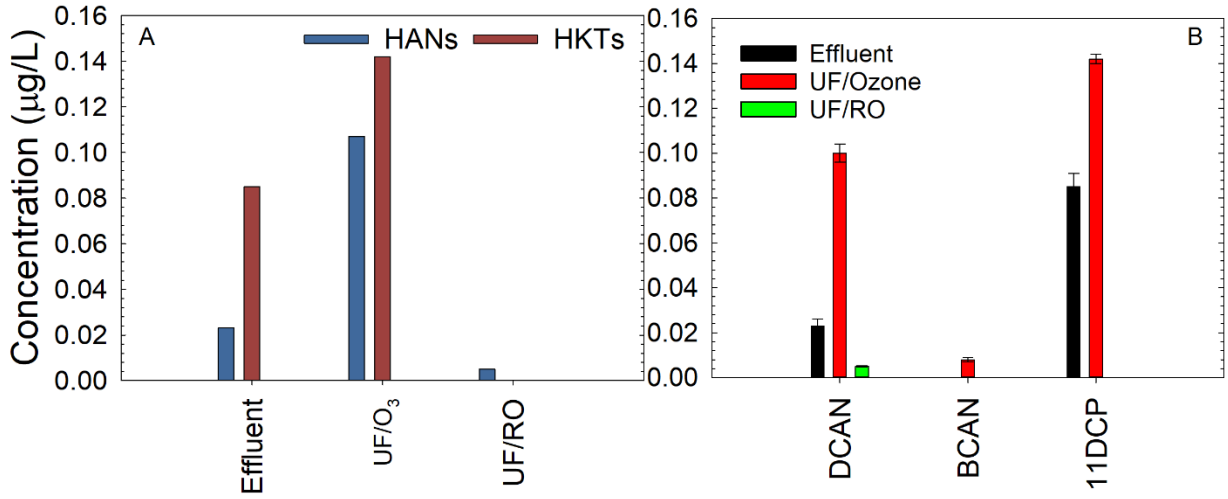

Figure 3-2: Quantified DBPs in secondary wastewater effluents (Effluent), ozonation (UF/Ozone), and reverse osmosis (UF/RO). DBPs are plotted **A)** by chemical classes, and **B)** individually by sample. Error bars represent the standard deviation of three replicate extractions.

3.3.2 Summer 2019: DBP Formation Potential with Chlorine

All water samples were chlorinated following the UFC procedure. A total of 12 DBPs were quantified after chlorination (Figure 3-3C). At least one DBP was quantified from all five classes in this method (HANs, I-THMs, HNMs. HKTs, and HALDs).

Wastewater secondary effluents produced the highest formation of DBPs in the order of HANs >> HALDs > HKTs > I-THMs > HNMs (Figure 3-3A). Specifically, DCAN was the largest forming DBP in secondary effluents at 27.05 µg/L. DCAN formation potential with chlorine disinfection was significant in secondary effluents which indicates that DCAN precursors are high. The second largest forming DBP was BDCAld at a concentration of 1.48 µg/L. Overall, a total of 30.8 µg/L of DBPs in this method formed after 24 hours, where DCAN and BDCAld constituted 87.8% and 4.8% of the total DBP makeup, respectively. Overall, the predominant formation of DCAN from chlorinated effluents has been observed in multiple studies where wastewater effluents were chlorinated for 24 hours. [82, 83] One study found that after 24 hour chlorination of secondary effluents, approximately 14.3 µg/L of DCAN formed, constituting the largest forming HAN in their method, which is consistent with our results. [82]

UF/O_3/HOCl effluents resulted in the second largest DBP forming water matrix with a total concentration of 12.95 µg/L were DCAN constituted 81.8% of the total DBP speciation (Figure 3-3C). The HAN class also comprised of TCAN, CAN, and BAN, although these DBPs comprised 3.13, 1.64, and 1.83%, respectively. Overall, the pre-ozonation step was able to reduce the total HAN concentration by 15.0 ug/L, indicating that precursors specific to HAN formation are readily degraded by ozone. Furthermore, the presence of a pre-ozonation step led to an increase in HNM formation post-

disinfection. The second largest forming DBP was BCNM at 1.22 µg/L (7.72%) in UF/O_3/HOCl effluents. Both HAN and HNM are nitrogenous DBPs that have been shown to form at greater concentrations in the presence of nitrogenous precursors typically found in EfOM. [84-86] Furthermore, the total nitrogen (TN) concentration of UF/O_3 quantified at 7.99 mg/L (Table 3-1) may have played a role in the predominant N-DBP formation observed in the UF/O_3/HOCl effluents.

Lastly, UF/RO/HOCl effluents produced the least amount of DBPs with a total concentration of 0.90 µg/L (Figure 3-3B). DCAN was the predominant DBP formed, comprising 37.0% of total DBP speciation (0.33 µg/L). Overall, the RO system was able to remove almost all DOC and ammonia nitrogen. TN was quantifiable at 0.44 mg/L (Table 3-1) which likely plays a role in such a significantly less DBP formation observed.

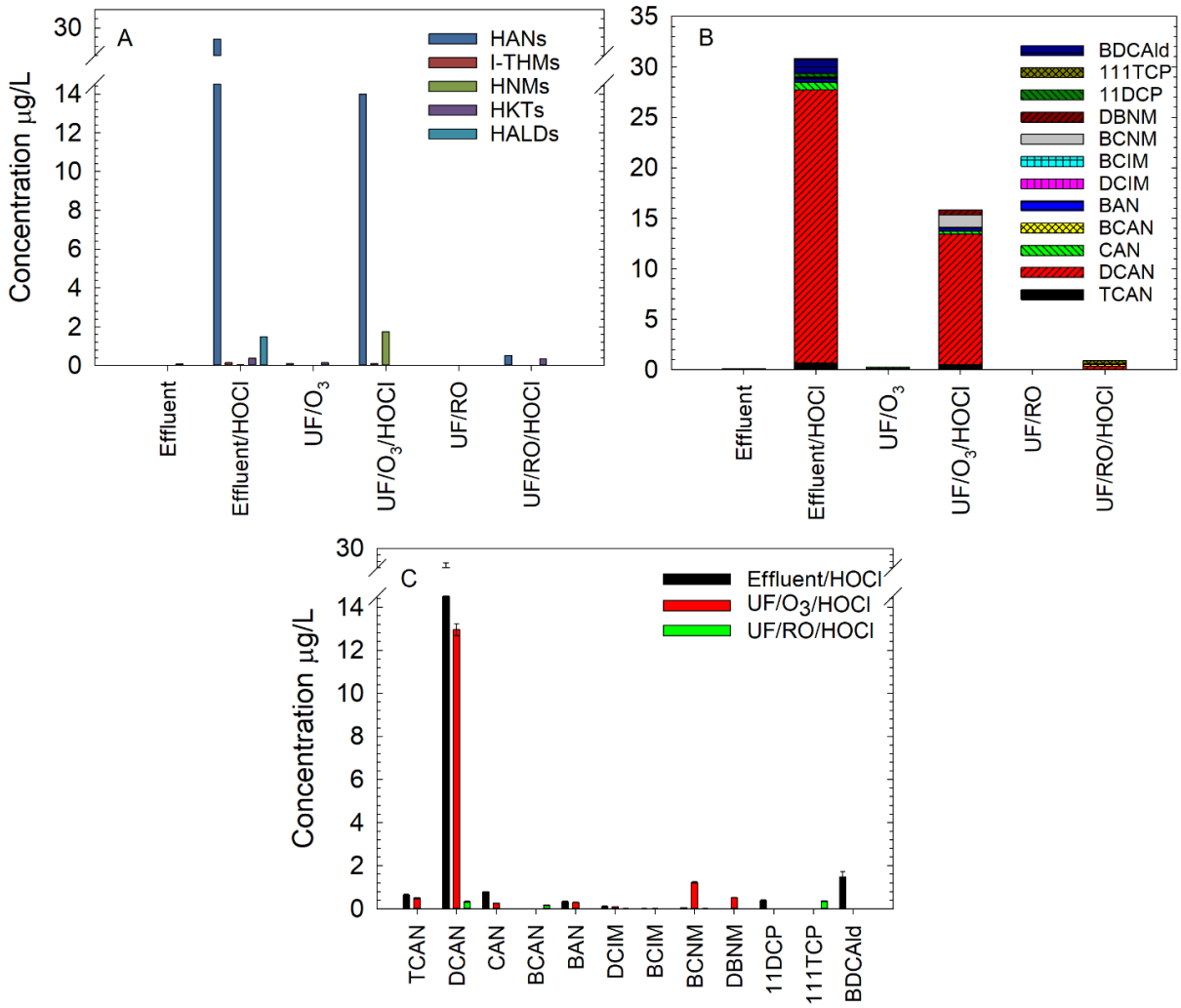

Figure 3-3: Quantified DBPs after chlorination of secondary wastewater effluents (Effluent/HOCl), microfiltration (UF/HOCl), and reverse osmosis (UF/RO/HOCl). DBPs are plotted **A)** by chemical classes, **B)** individually stacked by sample, and **C)** individually. Error bars represent the standard deviation of three replicate extractions.

3.3.3 Summer 2019: DBP Formation Potential with Monochloramine

DBP formation potential with chloramines produced HANs, I-THMs, HNMs, and HKTs, as noted in Figure 3-4A. Unlike chlorination, HKTs was the largest forming group upon chloramination. Specifically, HKTs only produced 0.37 µg/L in effluent/HOCl samples (Figure 3-3A), whereas 1.33 µg/L HKT formed in effluent/NH_2Cl samples (Figure 3-4A). Interestingly, HALDs were not formed during chloramination, however they did form during chlorination in effluent/HOCl samples at 1.47 µg/L (Figure 3-3A). Also, I-THMs formed at comparable concentrations in both chlorinated and chloraminated waters (Figure 3-3A, Figure 3-4A).

Effluent/NH_2Cl samples formed the second largest total DBP after UF/O_3/NH_2Cl. Specifically, 11DCP was the largest forming DBP at 1.33 µg/L in effluent/NH_2Cl. The second largest DBP formed was DCNM at a concentration of 0.12 µg/L in effluent/NH_2Cl waters. DCIM and BCIM also formed at concentrations ranging between 0.04-0.09 µg/L.

The highest DBP forming water matrix was UF/O_3/NH_2Cl with a total DBP of 3.31 µg/L (Figure 3-4B). Similar to effluent/NH_2Cl samples, the largest forming DBP was 11DCP at 2.75 µg/L. The increase of HKTs is an expected finding, as ozonation has been shown to breakdown organic matter to lower molecular weight compounds. [86] Yang et al. evaluated DBPs from river water that contained high levels of treated effluent discharge from three wastewater treatment plants in China and found that chloramination of ozonated water produced HKTs, HANs, and HNMs. [86]

Similar to the results observed during chlorination of UF/RO/HOCl effluents, UF/RO/NH_2Cl samples produced the lowest concentration of all disinfected samples.

Only HAN and I-THMs were formed after chloramination. The largest forming DBP was DCIM at a concentration of 0.08 µg/L.

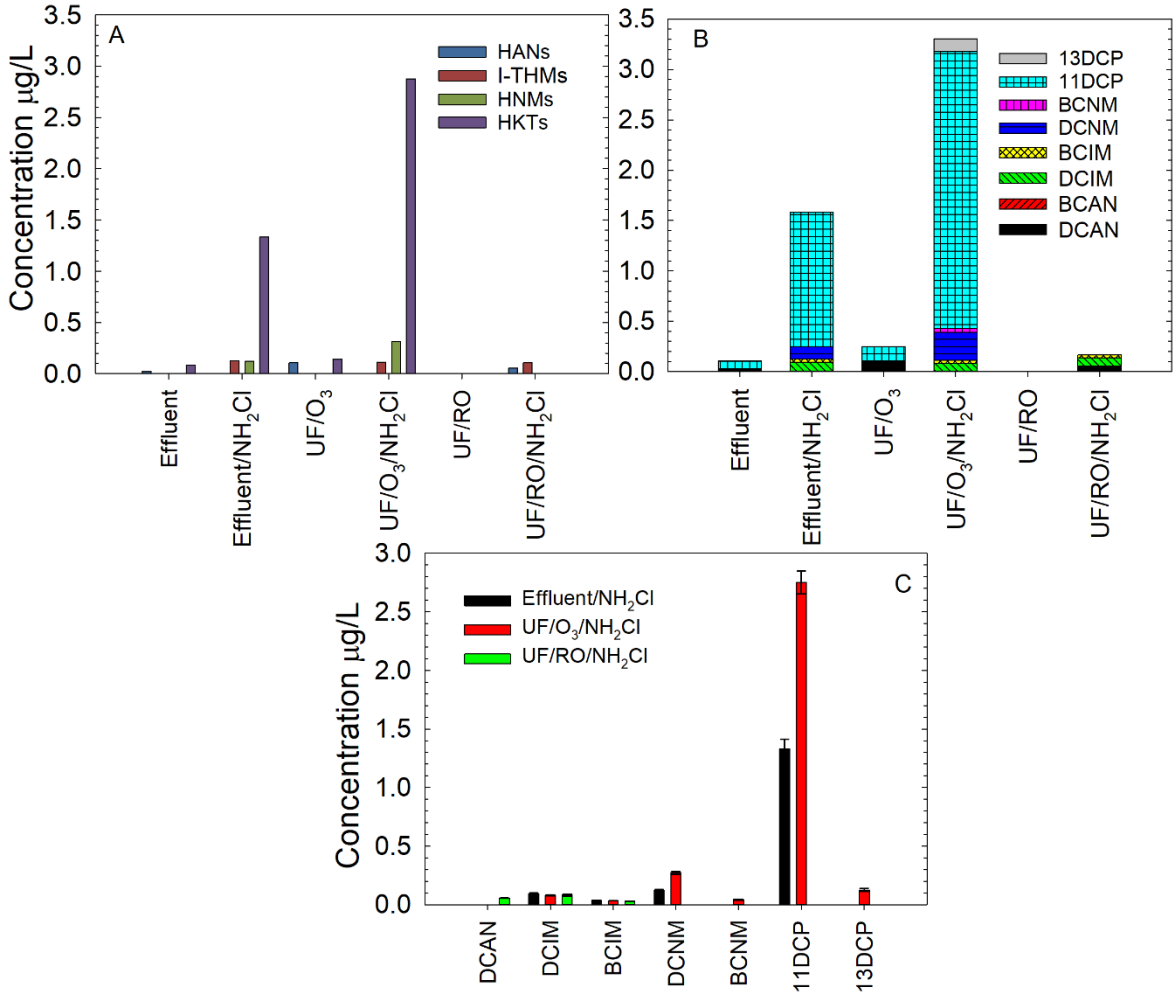

Figure 3-4: Quantified DBPs after chloramination of secondary wastewater effluents (Effluent/NH_2Cl), microfiltration (UF/NH_2Cl), and reverse osmosis (UF/RO/NH_2Cl). DBPs are plotted **A)** by chemical classes, **B)** individually stacked by sample, and **C)** individually. Error bars represent the standard deviation of three replicate extractions.

3.3.4 Fall 2019: DBPs in Advance Treatment of Secondary Wastewater Effluents

Water samples were collected from secondary wastewater effluents treated with microfiltration membranes (UF) followed by ozone (UF/O_3), and reverse osmosis (UF/RO). DBPs were quantified in all samples including CAN, DCAN, DCIM, BCIM, and DCNM (Figure 3-5B). DCAN and DCIM were quantified in secondary wastewater effluents at 14.8 and 13.3 ng/L, respectively and were subsequently reduced after UF treatment. In contrast, CAN and DCNM were not present in secondary effluents but were quantified after UF which suggests that CAN and DCNM were formed after UF.

UF/O_3 produced the highest DBP formation attributed primarily to HANs at 98.3 ng/L followed by I-THMs (29.6 ng/L). Although DCAN is reduced to 8.28 ng/L after UF treatment, it is re-formed after ozone treatment to a concentration of 90.3 ng/L. Non-halogenated and halogenated nitriles have been identified as a by-product in ozonation processes in drinking water. However, this is the first time DCAN formation has been observed from ozonation in a reuse treatment facility. The enhanced HAN formation after ozonation was not observed in two full-scale potable reuse facilities which might indicate that HAN formation could be unique to the composition of the effluent organic matter going through the facility in this study. [60]

After UF/RO treatment, DCAN, DCNM and DCIM levels were reduced between 14.7-43.4% compared to UF treatment alone. Additionally, BCIM was detected at 10.3 ng/L after UF/RO. A previous study that evaluated DBP rejection in RO membranes found that DCAN, DCIM and BCIM exhibited the lowest DBP rejection at steady state ranging

between ~40 – 50 %. [81] DBPs detected in this study also agree with a poor RO rejection as reported by Deoderer et al.

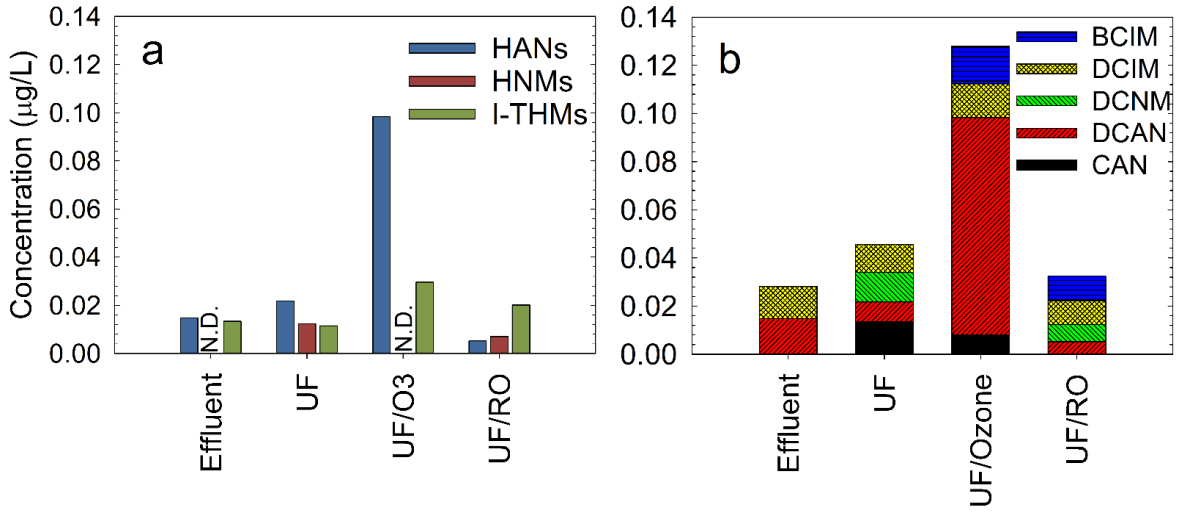

Figure 3-5: Quantified DBPs in secondary wastewater effluents (Effluent), microfiltration (UF), UF-ozonation (UF/Ozone), and reverse osmosis (UF/RO). DBPs are plotted **A)** by chemical classes, and **B)** individually stacked by sample.

Non-target analysis of the total organic halogen contained in water samples is shown in Figure 3-6. The largest organic halide was TOCl with an average of 102.4 and 122.4 µg/L as Cl^- in secondary effluent and UF samples, respectively. Ozone and RO treatment removed 64.3 and 86.4% of TOCl compared to UF-treated samples. However, TOBr and TOI concentrations were consistent (6.6-7.0 µg/L as Br^- and 3.1-9.5 µg/L as I^-) in secondary effluent, UF, and UF/O_3 samples. UF/RO samples had no detectable TOBr and TOI but TOCl was still observed after UF/RO treatment. These results suggest the presence of halogenated organic contaminants such as pharmaceuticals and personal care products that are not well removed from wastewater secondary treatment and advanced treatment processes. [87, 88]

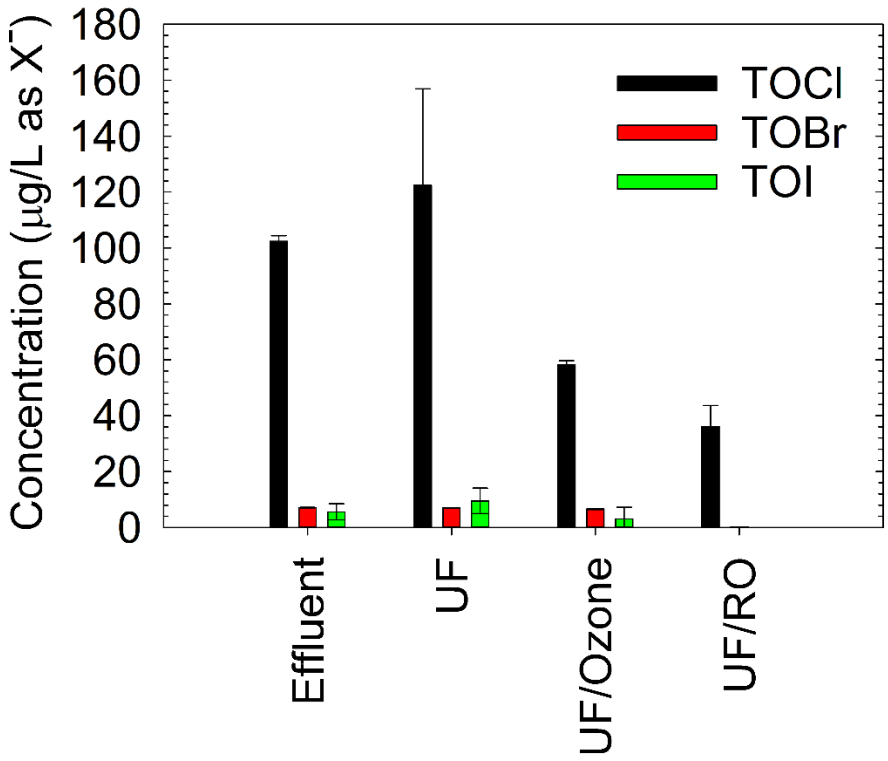

Figure 3-6: Total organic halogen obtained from water samples without disinfection. TOCl, TOBr, and TOI are expressed in µg/L as Cl^-, Br^- and I^-, respectively. Analysis were performed in triplicate and results are shown as the mean and standard deviation.

3.3.5 Fall 2019: DBP Formation Potential with Chlorine

Water samples were chlorinated according to UFC protocol to evaluate DBP formation potential and precursor removal of each treatment. A total of 12 of 25 DBPs were detected including HANs, I-THMs, HNMs, and HALDs as shown in Figure 3-7A. HKTs were not observed in any of the chlorinated samples. Secondary wastewater effluents and UF-treated waters had the highest DBP concentrations (Figure 3-7A) in the order of HANs >> HNMs > HALDs > I-THMs. DBP speciation was found to be similar for both chlorinated samples which correlated with dissolved organic carbon and total nitrogen concentrations (Table 3-1). One possibility is that filtering secondary wastewater

effluents in the laboratory may have produced similar matrix/precursor composition to UF samples. Another possibility was that the UF membranes were not performing adequately at the time of sampling. However, ACWA quantified DOC on the same month as sampling and reported 8.46 and 6.76 mg/L as carbon (C) for secondary wastewater effluent and UF treated samples, respectively. Therefore, sample prep filtration was the most likely explanation for similar DBP speciation for secondary wastewater effluent and UF samples. DCAN was the highest DBP with 12.9 and 13.7 µg/L in secondary wastewater effluents and UF treated waters, respectively. BCAN was the second highest DBP at a concentration of 2.92 and 2.96 µg/L for secondary wastewater effluents and UF, respectively. Additionally, total HNM, HAL and I-THMs levels were similar in secondary wastewater effluents and UF treated samples. Chlorinated effluent and UF samples formed 0.40-0.38 µg/L HNMs, 0.36-0.37 µg/L HALs, and 0.15-0.17 µg/L I-THMs.

UF/O_3/HOCl treated samples produced less DBPs compared to UF/HOCl (Figure 3-7A). However, total HAN (7.3 µg/L) was still the largest DBP chemical class with two major contributors, DCAN and BCAN that accounted for 77% (5.6 µg/L) and 18% (1.3 µg/L) of HAN formation, respectively. In comparison, ozonated water samples produced 42% less HANs than those quantified in UF-treated waters. These results suggest that ozonation is oxidizing amine precursors that lead to HAN formation. Similarly, other studies have also found that pre-ozonation followed by chlorination of effluent organic matter (EfOM) can decrease the formation of HANs with a simultaneous increase of HNM formation. [84-86] In our study, HNMs was the second largest DBP group with a total concentration of 3.8 µg/L where DCNM and BCNM accounted for 95% of the total. McCurry et al. proposed that ozonation can convert primary and secondary amines to

nitroalkanes, which can subsequently react with chlorine to form HNMs. [85] I-THMs were produced at significant lower levels than other DBP classes at 176.8 ng/L where DCIM accounted for ~90% of the total. I-THMs levels were similar to chlorinated secondary wastewater effluents and UF samples. Unexpectedly, HKTs and HALDs were not observed from UF/O_3/HOCl samples which might be related to the water's EfOM composition. A study conducted by Yang et al. found that pre-treatment with ozonation followed by chlorination of wastewater-impacted river waters enhanced the formation of haloketone 1,1,1-trichloropropanone (111TCP) and HALDs. [86]

UF/RO/HOCl samples exhibited significantly less DBP formation compared to the other treatments. This could in part be due to the lower DOC concentration in the sample (Table 3-1). RO was able to remove >85% of DOC which led to a lower DBP formation. Halonitromethanes were the most significant DBPs observed for chlorinated RO samples with DCNM and BCNM concentrations of 189 and 157 ng/L, respectively. HANs were also detected with concentrations of 52.5 and 53.1 ng/L for DCAN and BCAN, respectively. I-THMs were also observed with a total concentration of 26.3 ng/L (Figure 3-7C).

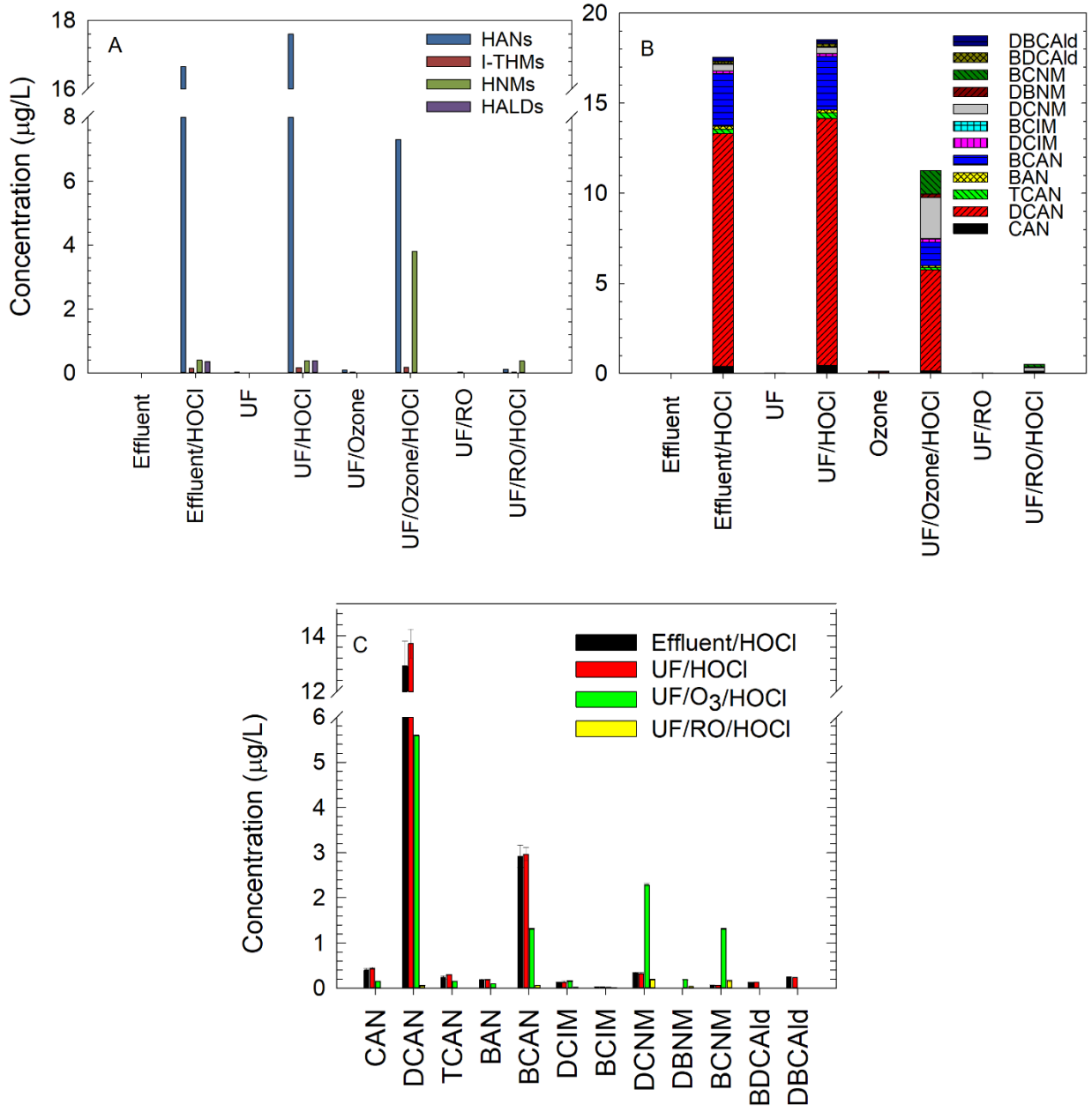

Figure 3-7: Quantified DBPs after chlorination of secondary wastewater effluents (Effluent/HOCl), microfiltration (UF/HOCl), ozonation (UF/O_3/HOCl), and reverse osmosis (UF/RO/HOCl). DBPs are plotted **A)** by chemical classes, **B)** individually stacked by sample, and **C)** individually. Error bars represent the standard deviation of three replicate extractions

3.3.6 Fall 2019: DBP Formation Potential with Monochloramine

Chloramination of collected waters produced HANs, I-THMs, HNMs, and HKTs as shown in Figure 3-8A. HAN formation was significantly lower for chloraminated wastewater, UF, and UF/O_3 samples (0.33-0.55 µg/L) compared to chlorination (0.1-18 µg/L). Unlike chlorinated samples, chloramination enhanced HKT formation and HALDs however, HALDs were detected below their MDLs. Additionally, an increased I-THMs formation was observed after UF/O_3 and UF/RO compared to UF treated samples.

Secondary effluents and UF-treated waters exhibited similar DBP speciation trends and concentrations. 1,1-dichloropropanone (11DCP) was the highest DBP formed in both waters with concentrations between 0.99-1.02 µg/L (Figure 3-8C). DCAN was the second largest DBP for both waters ranging 0.33-0.34 µg/L. Similar trends were observed in Linge et al. study that detected 11DCP and DCAN in chloraminated secondary effluent and UF waters. [59] Other DBPs detected include DCIM, BCIM, and DCNM with concentrations between 0.009-0.08 µg/L (Figure 3-8C).

UF/O_3-treated waters however, produced the highest DBP levels of all samples when disinfected with chloramines (Figure 3-8C). These results suggest that ozonation increases precursors that lead to a higher DBP formation. After a 24-hour chloramination, ozonated waters formed a total HNM concentration of 4.25 µg/L that included 4.05 µg/L DCNM and 0.20 µg/L BCNM. Song et al. also observed high HNM formation when secondary effluents underwent chloramination and ozonation-chloramination. [89] The pre-ozonation step resulted in a larger increase in HNMs consistent with this study. HKTs were the second largest forming DBP chemical class with a total concentration of 2.97 µg/L (Figure 3-8A) composed by 11DCP and 1,1,1-Trichloropropanone (111TCP). Total

HAN (0.56 µg/L) increased after UF/O_3/NH_2Cl compared to UF/NH_2Cl treated samples which included DCAN and BCAN. The increased formation of HANs in pre-ozonated waters is unexpected, as previous studies have shown that the pre-ozonation step reduced HAN precursors. [71, 86, 90] However, Yang et al. showed that waters with elevated bromide levels displayed an increase in HAN formation in pre-ozonated waters. [86] In this study, the UF/ozone water sample had 39.6 µg/L bromide which may have led to the formation of BCAN and therefore, an increase in HAN concentration. I-THMs in UF/O_3/NH_2Cl waters produced ~4x more I-THMs compared to UF/O_3/HOCl. It is well known that iodide in the presence of monochloramine can form HOI which can further react to produce I-THMs. [91, 92] However, chlorine and ozone can readily oxidize hypoiodous acid (HOI) to iodate, a non-toxic iodine sink, that minimizes the formation of I-THMs. Furthermore, I-THMs were ~22x higher in UF/O_3/NH_2Cl waters than UF/NH_2Cl waters. These results indicate that iodine precursors might have been in the form of organic iodine (Figure 3-8A) instead of free iodide. Ozone can oxidize organic matter and increase I-THM precursors that subsequently react with chloramine to primarily form iodoform (TIM), followed by DCIM, CDIM, and BCIM. The tri-substituted TIM present in UF/O_3/NH_2Cl waters indicate that a relative high concentration of HOI oxidized organic matter multiple times, leading to a high TIM concentration.

Similar to UF/RO/HOCl samples, UF/RO/NH_2Cl samples formed the least amount of DBPs compared to other treatments because of the efficient DOC removal by RO. Of all DBP classes formed, I-THMs was the largest DBP class attributed to DCIM with a concentration of 107 ng/L as seen in Figures 3-8C. DCNM and DCAN were formed at

similar levels at 29.9 and 27.3 ng/L, respectively and were the only HAN and HNM detected in these chloraminated waters.

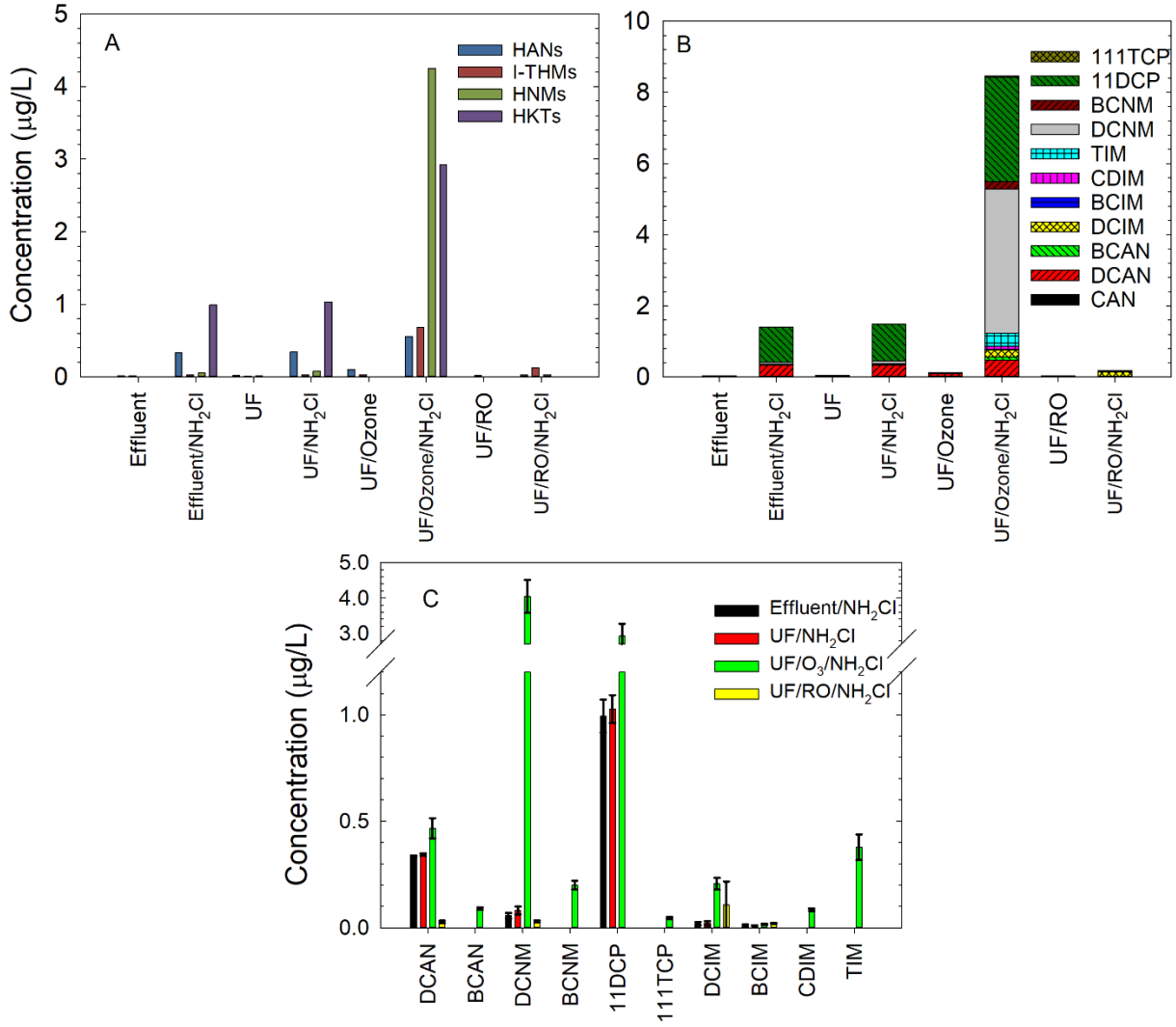

Figure 3-8: Quantified DBPs after chloramination of secondary wastewater effluents (Effluent/NH_2Cl), microfiltration (UF/NH_2Cl), ozonation (UF/O_3/NH_2Cl), reverse osmosis (UF/RO/NH_2Cl). DBPs are plotted **A)** by chemical classes, **B)** individually stacked by sample, and **C)** individually. Error bars represent the standard deviation of three replicate extractions

3.3.7 Winter 2020: DBPs in Advance Treatment of Secondary Wastewater Effluents

A third sampling event was conducted in the winter months where effluent, UF, UF/O_3, and UF/RO were analyzed for DBPs. A total of 7 DBPs were quantified including TCAN, DCAN, CAN, BCIM, DCIM, DCNM, and 111TCP (Figure 3-9 B,C). The largest forming DBPs in secondary effluent were DCAN, DCIM, and 111TCP at 20.4 ng/L, 19.9 ng/L, and 24.5 ng/L, respectively. Of these DBPs, both DCAN and DCIM were reduced after the UF process at 15.3 ng/L and 11.87 ng/L, respectively (Figure 3-9C). 111TCP, however, remained at the same concentration at 24.5 ng/L after passing through the UF system. All DBPs quantified in secondary effluent (CAN, DCAN, BCIM, DCIM, DCNM, and 111TCP) decreased or remained at the same concentration after passing through UF except CAN (Figure 3-9C). CAN was quantified in secondary effluent at 8.65 ng/L and subsequently increased to 10.63 ng/L after UF processes.

UF/O_3 effluents produced the greatest amount of DBPs, including CAN, DCAN, TCAN, BCIM, DCIM, DCNM, and 111TCP. Of these DBPs, the HAN class was the highest forming DBP class where DCAN accounted for 85.01% of the HAN composition (Figure 3-9A,C). Similar to secondary effluents, UF/O_3 largest forming DBPs were DCAN, DCIM and 111TCP at 58.86 ng/L, 20.04 ng/L, and 32.74 ng/L, respectively. After UF/O_3 treatment, DCAN was the largest increase in DBP formation after UF treatment (Figure 3-9B,C). DCAN concentration decreased after UF treatment, however, upon ozonation the concentration increased from 15.3 ng/L to 58.86 ng/L. It is well known that ozonation produces HANs, however, this sampling is consistent with the summer and fall 2019 sampling events where both DCAN and 111TCP experienced a significant formation after

ozonation. This further supports the hypothesis that Calgary wastewaters contain precursors that lead to the formation of DCAN when undergoing advanced oxidation. [60]

Following UF/RO treatment, DCAN and 111TCP were both experienced a 100% reduction from the sample matrix. Interestingly, DCIM and BCIM concentration almost doubled in concentration from 9.7 ng/L and 11.86 ng/L to 18.98 ng/L and 24.39 ng/L, respectively. These results indicate that there are reactions occurring at the UF/RO that lead to the formation of I-THMs. Allard et al. conducted a similar study where I-THMs were quantified in secondary effluents and post – ultrafiltration/pre reverse osmosis effluents. Their results show that following the ultrafiltration step, DCIM was detectable. This detection further supports our hypothesis that DCIM forms along the treatment train. [93]

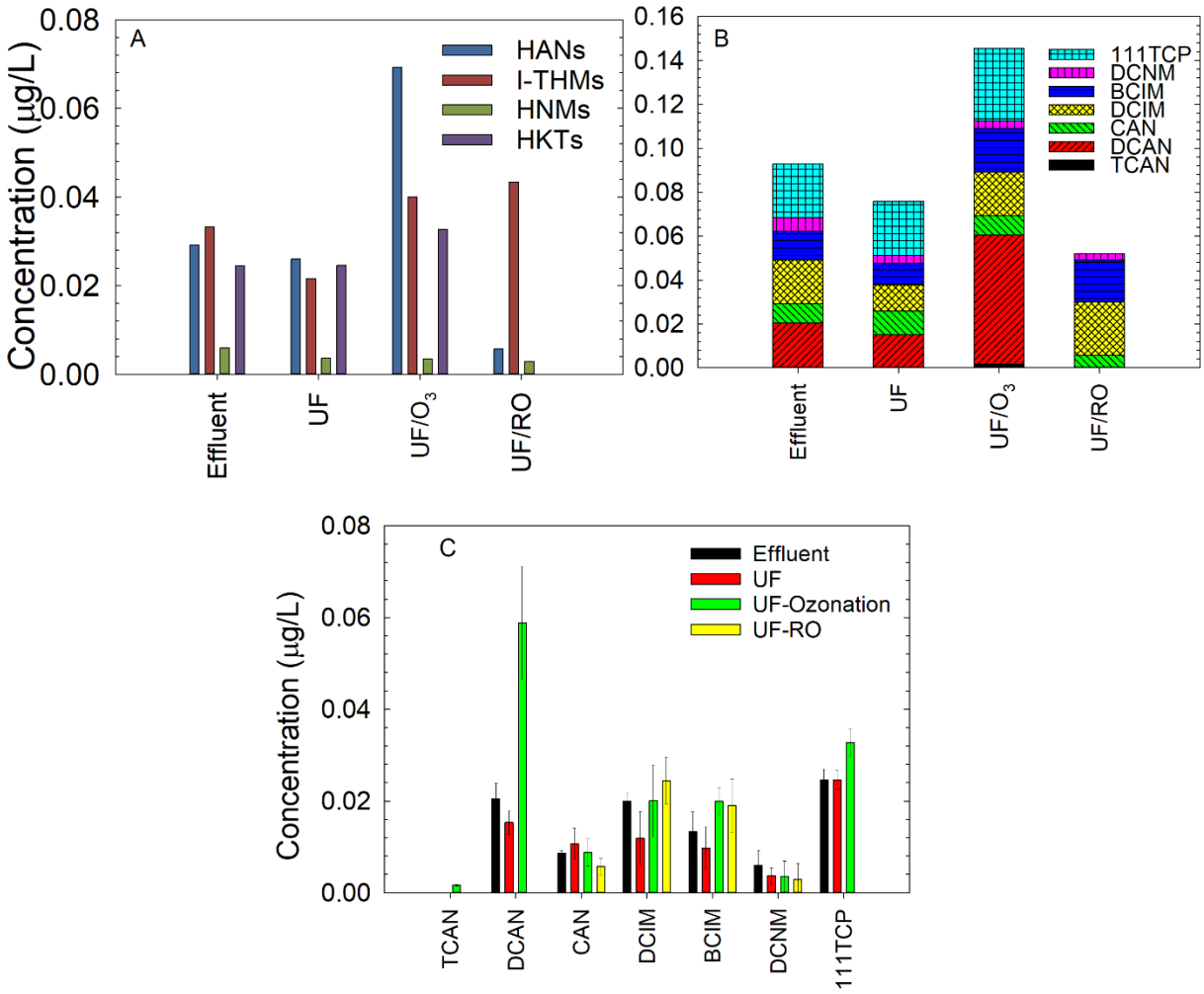

Figure 3-9: Quantified DBPs in secondary wastewater effluents (Effluent), microfiltration (UF), UF-ozonation (UF/Ozone), and reverse osmosis (UF/RO). DBPs are plotted **A)** by chemical classes, **B)** individually stacked by sample, and **C)** individually by sample. Error bars represent the standard deviation of three replicate extractions.

TOX analysis was performed for all water samples as seen in Figure 3-10. TOCl was the largest halide quantified at 97.69 µg/L and 99.40 µg/L in effluent and UF samples, respectively. UF/O_3 and UF/RO samples removed approximately 26.75 % and 94.57% of TOCl from UF samples, respectively. TOBr remained somewhat consistent in effluent, UF

and UF/O_3 samples at 6.75 µg/L, 6.83 µg/L, and 4.56 µg/L, respectively. However, upon UF/RO filtration, TOBr was below the detection limit. [87, 88] Interestingly, October's TOX analysis revealed the presence of TOI in all effluents except UF/RO. TOCl and TOBr level were quantified at comparable concentrations, however, February's samples did not show any detected TOI.

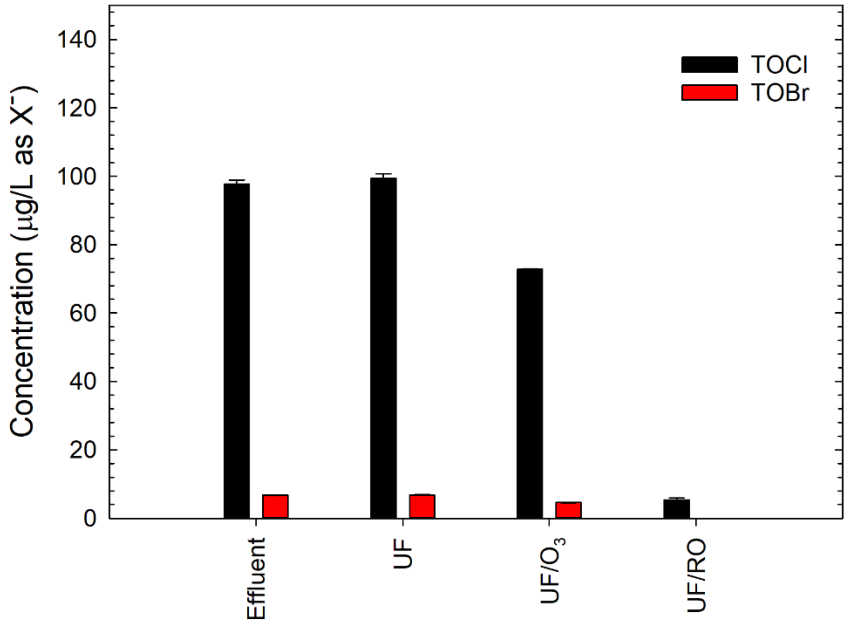

Figure 3-10: Total organic halogen obtained from water samples without disinfection. TOCl, and TOBr are expressed in µg/L as Cl^-, and Br, respectively. Analysis were performed in triplicate and results are shown as the mean and standard deviation

3.3.8 Winter 2020: DBP Formation Potential with Chlorine

All water samples were chlorinating following the same UFC procedure for all sampling events. After 24 hr disinfection, a total of 15 of 25 DBPs were quantified. Every class of DBP in this method was formed after disinfection including HANs, I-THMs, HNMs, HKTs, and HALDs (Figure 3-11A). In comparison to summer and fall 2019 sampling events, this sampling event produced the largest amount of DBPs. Furthermore, chlorination of secondary effluent matrices in winter 2020 lead to the second largest sum of all DBP speciation (19.61 µg/L) compared to chlorinated samples from fall and summer 2019 at, 17.56 µg/L, and 30.82 µg/L in effluent/HOCl, respectively.

Effluent/HOCl and UF/HOCl water matrices lead to almost identical DBP speciation. This trend in DBP formation was observed across all sampling events. It was hypothesized that the pre-filtering step of the effluent and UF matrix lead to almost identical organic composition, thereby producing similar DBP speciation results. Of all DBPs formed, both effluent/HOCl and UF/HOCl lead to DCAN being the largest forming DBP at 13.54 µg/L and 12.53 µg/L, respectively. The second largest DBP class were the HKTs where 111TCP accounted for 1.96 µg/L and 2.75 µg/L in effluent/HOCl and UF/HOCl, respectively. Interestingly, UF/HOCl waters formed approximately 0.79 µg/L more of 111TCP and 0.020 µg/L of 1B11DCP (Figure 3-11C). Furthermore, February chlorination was the only sampling event where 1B11DCP was formed in UF matrices upon chlorination.

UF/O_3/HOCl treated waters in Winter 2020 produced the largest forming DBPs across all sampling events leading to a total sum of 34.97 µg/L of all DBPs. Specifically, 14.29 µg/L, almost 46% was attributed to 11DCP. The second largest HKT was attributed

to the formation of 111TCP and 1B11DCP at concentrations of 6.70 µg/L and 0.028 µg/L, respectively (Figure 3-11C). A similar study found that wastewater-impacted river waters pre-treated with ozonation followed by chlorination increased the formation of haloketone 1,1,1-trichloropropanone (111TCP) and HALDs. The second largest DBP was DCAN with a concentration of 8.63 µg/L in UF/O_3/HOCl treated waters. DCAN was one of the largest forming DBPs across all sampling events as well as all water matrices, regardless of HOCl and NH_2Cl being the disinfectant in use. [86]

UF/RO/HOCl followed typical trends across all sampling events resulting in the lowest formation of all DBPs, regardless of disinfectant. DCAN was the largest contributor to the total DBP concentration accounting for 0.111 µg/L in treated RO waters.

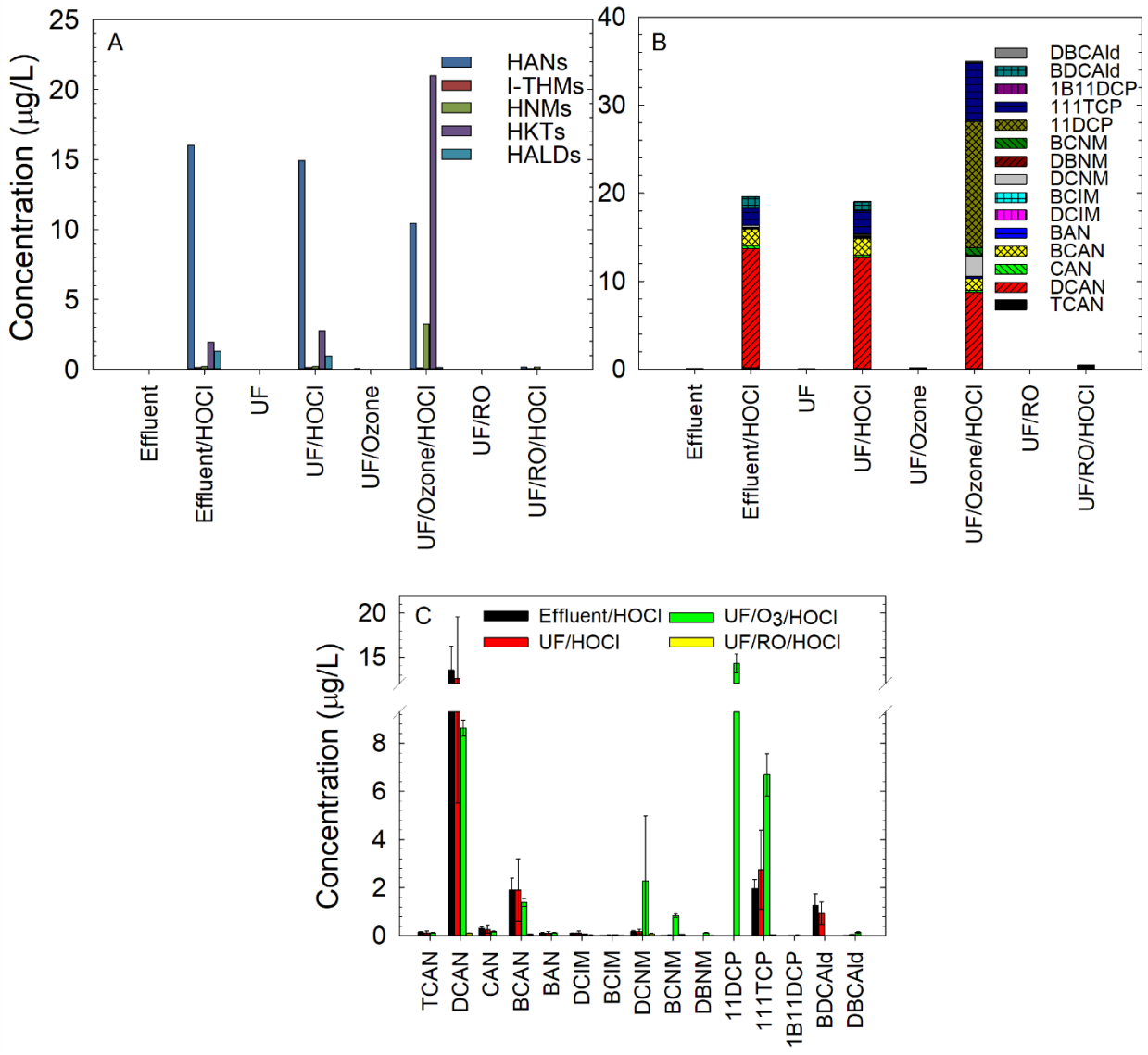

Figure 3-11: Quantified DBPs after chlorination in secondary wastewater effluents (Effluent/HOCl), microfiltration (UF/HOCl), UF-ozonation (UF/Ozone/HOCl), and reverse osmosis (UF/RO/HOCl). DBPs are plotted **A)** by chemical classes, **B)** individually stacked by sample, and **C)** individually by sample. Error bars represent the standard deviation of three replicate extractions.

Non – targeted TOX analysis was ran on all disinfected waters as shown in Figure 3-12. TOCl was the largest organic halide with concentrations of 91.83 µg/L, and 86.97

µg/L in effluent/HOCl and UF/HOCl, respectively. After UF/O_3/HOCl, TOCl dropped 67.34 µg/L which was approximately a 22.6 % TOCl reduction. UF/RO/HOCl waters contained 4.52 µg/L of TOCl. Reverse osmosis membranes reduce TOCl well over 99.9%. TOBr was also quantified in all chlorinated water matrices at 6.35 µg/L, 5.99 µg/L, 4.23 µg/L in Effluent/HOCl, UF/HOCl, and UF/O_3/HOCl, respectively. TOBr was not detected in UF/RO/HOCl waters. [87, 88]

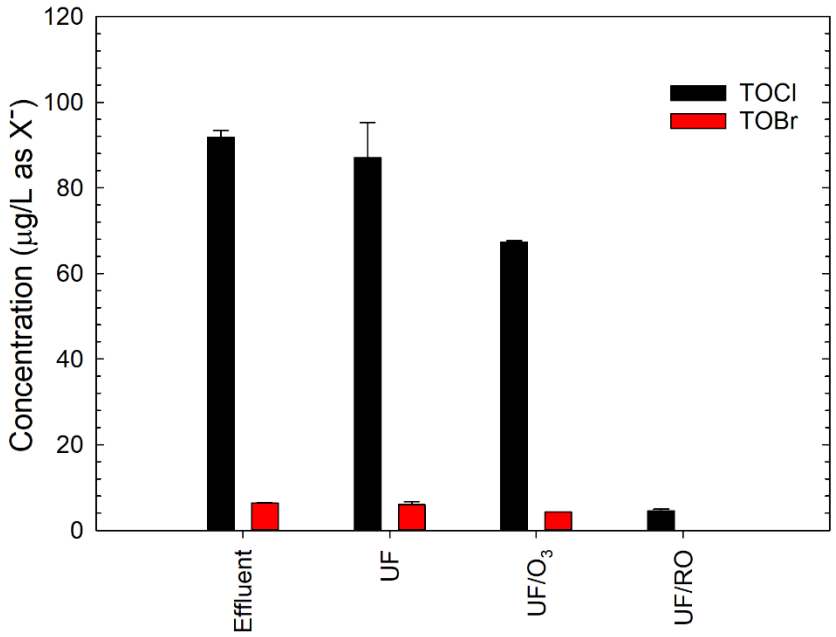

Figure 3-12: Total organic halogen obtained from water samples with chlorination. TOCl, and TOBr are expressed in µg/L as Cl^-, and Br, respectively. Analysis were performed in triplicate and results are shown as the mean and standard deviation.

3.3.9 Winter 2020: DBP Formation Potential with Monochloramine

All samples were collected and chloraminated following the same UFC protocol for previous sampling events. Chloraminated samples produced a total of 9 of the 25 DBPs validated in this method, where HANs, I-THMs, HNMS, HKTs, and HALDs all formed after

24 hr. HANs were the largest forming class in Effluent/NH_2Cl and UF/ NH_2Cl (Figure 3-13A). UF/O_3/NH_2Cl treated effluents largest DBP class were the HNMs, and UF/RO/NH_2Cl formed I-THMs as the largest DBP class after disinfection (Figure 3-13A).

Effluent/NH_2Cl and UF/NH_2Cl treated effluents had almost identical DBP speciation. This trend was noted across all sampling events, regardless of disinfectant (Figure 3-4, 3-8, 3-13). HANs were the largest DBP class where DCAN accounted for 0.228 µg/L (93.10%) and 0.256 µg/L (93.59%) in effluent/NH_2Cl and UF/NH_2Cl treated, respectively (Figure 3-13C). Primarily forming DCAN trends were also observed in a similar study where DBP characterization of HANs were done on treated effluents by Linge et al. [59] DCNM was the second largest forming DBP in Effluent/NH_2Cl and UF/NH_2Cl with concentrations of 0.044 µg/L and 0.058 µg/L, respectively. DCIM and BCIM speciation were also quantified in winter 2020 with concentrations ranging between 0.021-0.032 µg/L, similar values to the fall 2019 sampling event.

UF/O_3/NH_2Cl samples produced the largest concentration of all classes of DBPs. These results are in agreement with the previous chloraminated sampling events with pre-ozonation. Both summer and fall 2019 chloraminated UF/O_3/NH_2Cl effluents resulted in the largest DBP speciation. Specifically, HNMs were the largest forming DBP class for winter 2020 disinfection (Figure 3-13A) with a summed concentration of 1.464 µg/L. This trend was also observed in the October 2019 sampling event, however, the HNM class formed a total of 4.250 µg/L after 24 hr disinfection (Figure 3-8C). DCNM was the largest forming HNM in winter 2020 constituting 94.48% of the total HNM concentration (Figure 3-12A,C). Song et al also observed increased HNM concentrations after chloramination of ozonated effluents. [89] The second largest DBP class were the HANs with a total

concentration of 0.382 µg/L as seen in Figure 3-13A. DCAN, CAN and BCAN were formed after chloramination where 93.59 % of the HAN concentration was attributed to DCAN with a concentration of 0.357 µg/L. It is unusual that HANs continue to form at relatively large concentrations in pre-ozonated waters as studies have shown that ozonation reduces HAN precursors. [71, 86, 90] However, this trend has been observed fall 2019 sampling event, but not during the summer 2019 sampling event, indicating that there might be an effect of seasonality which influences the formation of HANs in UF/O_3/NH_2Cl chloraminated effluents (Figure 3-8A,C and Figure 3-13A,C). Lastly, this was the only sampling event that lead to detectable levels of HALDs. A total of 0.118 µg/L (100% HALDs) of DBCAld was formed in UF/O_3/NH_2Cl samples (Figure 3-13A,C). HKTs and I-THMs also formed in UF/O_3/NH_2Cl treated waters with levels ranging between 0.012-0.031 µg/L as seen in Figure 3-13A.

UF/RO/NH_2Cl treated waters produced the least amount of unregulated DBPs. The largest forming DBP class were the I-THMs which had a total concentration of 0.088 µg/L which comprised of DCIM (62.30%) and BCIM (37.70%) as seen in Figure 3-13A. These results are comparable to UF/RO/HOCl I-THM formation with a total concentration of 0.062 µg/L. Similarly, DCIM was the largest forming I-THM, accounting for 51.56% and BCIM accounted for 48.44% (Figure 3-11A).

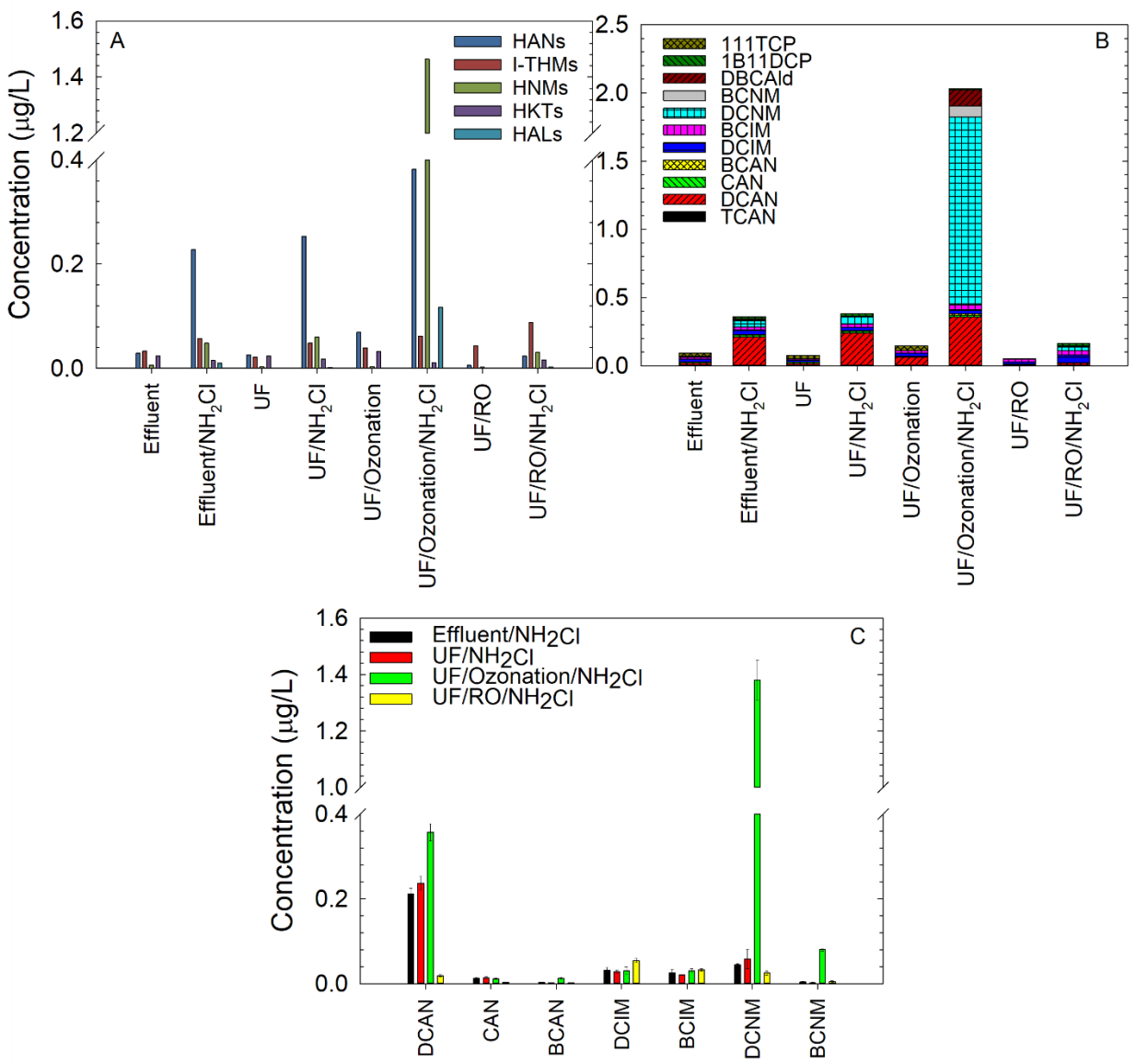

Figure 3-13: Quantified DBPs after chloramination of secondary wastewater effluents (Effluent/NH_2Cl), microfiltration (UF/NH_2Cl), ozonation (UF/O_3/NH_2Cl), reverse osmosis (UF/RO/NH_2Cl). DBPs are plotted **A)** by chemical classes, **B)** individually stacked by sample, and **C)** individually. Error bars represent the standard deviation of three replicate extractions

TOX analysis was conducted to determine the TOCl, TOBr, and TOI values after 24 hr chloramination. TOCl was the largest organohalogen in both effluent/NH_2Cl and UF/NH_2Cl at 157.38 and 161.77 µg/L, respectively. Ozonated effluents contained 140.62 µg/L of TOCl (Figure 3-14). TOCl values increased across effluent, UF, and ozonated effluents after chloramination. TOI was not detected in any of the water samples before disinfection, however, after chloramination, TOI was detected in secondary effluent, UF, and ozonated waters at 1.55 µg/L, 0.52 µg/L, and 0.13 µg/L, respectively (Figure 3-14). The formation of TOI is likely due to the oxidation of iodide to HOI in the presence of monochloramine, thereby iodinating organics present in the effluents. Iodide, however, was undetectable across all untreated effluents. The origin of the iodide is unknown but may likely be present below the MDL of the TOX method.

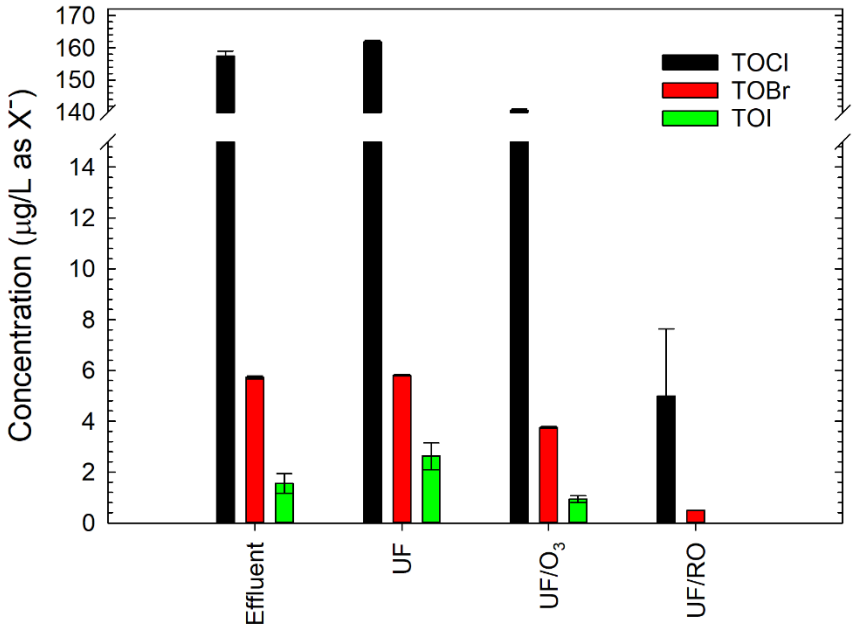

Figure 3-14: Total organic halogen obtained from water samples after chloramination. TOCl, TOBr, and TOI are expressed in µg/L as Cl^-, Br^- and I^-, respectively. Analysis were performed in triplicate and results are shown as the mean and standard deviation.

3.4 Conclusions

This study quantified DBP formation potential with chlorination and chloramination across three sampling events at ACWA. Samples were obtained from the same sampling ports for each water matrix to obtain comparable results across each event. Results detail the DBP formation potential of 25 high priority DBPs in a full-scale wastewater reuse facility.

During the first sampling event in summer 2019, secondary effluent, UF/Ozone, and UF/RO waters were sampled and extracted for DBP analysis prior to disinfection. Results demonstrated that HANs and a HKT were present before disinfection. Upon HOCl disinfection, effluent/HOCl, and UF/O_3/HOCl produced HANs as the largest DBP class comprising mainly of DCAN. UF/RO/HOCl produced the least amount of DBPs, where again, DCAN was one of the largest contributors. Chloramination of these wastewater effluents resulted in HKT and HNM classes being the largest contributors to the DBP composition in effluent/NH_2Cl, and UF/O_3/ NH_2Cl waters. Specifically, 11DCP and DCNM were the largest forming DBPs in these waters. Similar to chlorination, UF/RO/NH_2Cl formed the least amount of DBPs, however, I-THMs were the largest forming DBPs in this matrix.

The second sampling event in Fall 2019, several DBP formation trends observed in summer 2019 were repeated. Chlorinated recycled waters produced high levels of HANs (~18 µg/L) which was ~20x higher than chloraminated recycled waters. HALDs, I-THMs and HNMs were also detected. Pre-ozonation enhanced HNM formation in UF/O_3/HOCl waters. HANs and HNMs were the most predominant DBPs quantified in UF/RO/HOCl treated waters. Chloraminated recycled waters predominantly formed HKTs

however, when a pre-ozonation was applied (UF/O_3/NH_2Cl), HNMs were the largest forming DBP class. UF/O_3/NH_2Cl produced the highest DBP levels compared to other 3 treated waters. I-THM levels increased after UF/O_3/NH_2Cl and UF/RO/NH_2Cl treatment compared to UF/NH_2Cl treatment alone.

UF/O_3 had the largest concentration of DBPs present in effluents prior to chlorination or chloramination. Chlorinated effluents resulted in HKTs being the largest DBP class at ~20 µg/L followed with HANs in Effluent/HOCl, and UF/HOCl being the largest forming DBP class. Similar to previously observed trends, pre-ozonation enhanced the formation of HNMs and HANs in UF/O_3/NH_2Cl waters. Chlorinated and chloraminated UF/RO waters lead to predominantly HAN and I-THM speciation, respectively. The formation of I-THMs in chloraminated waters was a repeated trend across all sampling events for UF/RO/NH_2Cl waters.

Chapter 4: Conclusions and Future Directions

4.1 Conclusions

As climate change and population growth continue to affect freshwater sources, the need to obtain a sustainable drinking water alternative continues to persist. Potable wastewater reuse is an area in water treatment gaining momentum. The drawback of most approved analytical methods for DBP regulation is that they are validated for pristine water sources versus wastewater effluents. Moreover, many of these analytical methods lack trace level sensitivity to DBPs, which was accomplished in this work. Traditionally, the analytical methods quantitate regulated DBPs which have been shown to not be toxic in biologic systems. [5, 19] Therefore, one objective of this work was to develop an analytical method on a GC-MS/MS with trace level quantification of high priority unregulated disinfection by-products. GC-MS/MS parameters such as collision energies, dwell times, and chemical transitions were optimized to ensure low level MDLs. Trace level MDLs were obtained for all DBPs in this method ranging from 2.0-68.9 ng/L. Percent recoveries in ultra pure water and secondary effluents ranged between 31-104% and 29-83%, respectively. Furthermore, these optimizations enabled the full validation of this analytical method in wastewater effluents, which is a novel approach with a GC-MS/MS.

Secondly, this work characterized the efficacy of precursor removal from four wastewater effluents. Specifically, wastewater effluent, effluent/UF, UF/O_3, and UF/RO were disinfected with chlorine, and chloramines. Furthermore, DBP quantification was characterized in summer 2019, fall 2019, and winter 2020 along the same sampling ports. DBP quantification revealed the following results in regards to formation and concentration of the five DBP classes studied.

- HANs were the largest forming DBP class in Effluent/HOCl, UF/HOCl and UF/O_3/HOCl samples in every sampling event when chlorinated.
- DCAN was the largest forming HAN in in June, October and February in chlorinated Effluent/HOCl, UF/HOCl and UF/O_3/HOCl samples.
- Chloraminated effluents lead to the largest formation of 11DCP in all UF/O_3/NH_2Cl effluents in June, October and February sampling events. HNMs were also one of the largest forming class in chloraminated effluents with DCNM being the largest contributor.
- UF/RO/HOCl and NH_2Cl lead to the smallest formation of DBPs across all sampling events. Chlorination lead to primarily HAN formation, although HKTs and HNMs did form at trace levels in most sampling events. Chloramination of UF/RO effluents lead to primarily I-THM formation across all sampling events, however, HNMs formed as well.

The original objectives of this project were executed, however, further investigation can help bridge the knowledge gap that exists regarding mechanistic processes that lead to DBP formation.

4.2 Limitations

- The work described in sections 2.3.5, and 2.3.6 is not a formal optimization, but rather a modification of the previously used extraction method. These efforts were done in order to save time and reagents while ensuring the overall DBP recoveries were not significantly changed.
- A more thorough LLE optimization could be performed if analyte recovery was compared when all variables change at the same time. Specifically, this is

achieved by employing a design of experiments where a set of parameters are changing.

4.3 Future Work

4.3.1 Addition of Haloacetamides (HAMs) into DBP method

One area of improvement for this work would be the addition of haloacetamides (HAMs) to the DBP quantification method. Specifically, a beneficial goal would be to add chloroacetamide (CAM), bromoacetamide (BAM), iodoacetamide (IAM), dichloroacetamide (DCAM), chloriodoacetamide (CIAM), bromoiodoacetamide (BIAM), diiodoacetamide (DIAM), trichloroacetamide (TAM), bromodichloroacetamide (BDCAM), and tribromoacetamide (TBAM) to the method. Cuthbertson et al. recently published an analytical method that quantifies these DBPs on a GC-MS from finished drinking water samples. [32] Adding these unregulated DBPs would expand the number of N-DBPs which are the largest forming DBPs from wastewater effluents. Furthermore, adding HAMs would be a huge improvement to the method as previous studies have demonstrated the elevated toxicity associated with this class of DBPs. [12]

4.3.2 Drinking water UFC formation potential tests

An area that should be further studied is the quantification of finished drinking waters. While the aim of this work was to study the DBP composition of treated effluents, it would also be helpful to compare results from this study to those generated from treated drinking waters. Most GC-MS/MS methods for DBP quantification show that unregulated DBPs also exist in drinking water. Since this analytical method includes a comprehensive set of DBPs, it could shed more light on the unregulated DBP composition of Canadian drinking water quality. [31-34]

4.3.3 Characterizing EfOM precursor structure: FT-ICR-MS

Another area that should be further explored should be the characterization of EfOM with various technique including Fourier transform ion cyclotron resonance mass spectrometry (FT-ICR-MS) and fluorescence emission. FT-ICR-MS is option worth exploring due to the instrument being available at the University of Calgary. Furthermore, there are data scientists who are trained in complex data analysis associated with FT-ICR-MS. Specifically, by extracting EfOM from effluent, UF, UF/O_3, and UF/RO before disinfection, the chemical composition of DBP precursors can be detected by FT-ICR-MS by observing the change in parameters of hydrogen to carbon, double bond equivalents to carbon, and oxygen to carbon ratios in EfOM that lead to the formation of priority DBPs. [94]

References

1. Hoxie, N. J.; Davis, J. P.; Vergeront, J. M.; Nashold, R. D.; Blair, K. A., Cryptosporidiosis-associated mortality following a massive waterborne outbreak in Milwaukee, Wisconsin. *Am J Public Health* **1997,** *87* (12), 2032-2035.

2. Crittenden, J. C.; Trussell, R. R.; Hand, D. W.; Howe, K. J.; Tchobanoglous, G., *MWH's water treatment: principles and design*. John Wiley & Sons: 2012.

3. Snoeyink, L. V., Jenkins David *Water Chemistry*. John Wiley & Sons, Inc.: 1980; p 463.

4. Chu, W.; Gao, N.; Yin, D.; Krasner, S. W., Formation and speciation of nine haloacetamides, an emerging class of nitrogenous DBPs, during chlorination or chloramination. *Journal of hazardous materials* **2013,** *260*, 806-812.

5. Plewa, M. J.; Wagner, E. D., Charting a new path to resolve the adverse health effects of DBPs. In *Recent Advances in Disinfection By-Products*, ACS Publications: 2015; pp 3-23.

6. Richardson, S. D.; Plewa, M. J.; Wagner, E. D.; Schoeny, R.; DeMarini, D. M., Occurrence, genotoxicity, and carcinogenicity of regulated and emerging disinfection by-products in drinking water: a review and roadmap for research. *Mutation Research/Reviews in Mutation Research* **2007,** *636* (1-3), 178-242.

7. Guideline for Canadian drinking water quality, Ontario, Canada

8. Bond, T.; Huang, J.; Templeton, M. R.; Graham, N., Occurrence and control of nitrogenous disinfection by-products in drinking water–a review. *Water research* **2011,** *45* (15), 4341-4354.

9. Chang, H.; Chen, C.; Wang, G., Characteristics of C-, N-DBPs formation from nitrogen-enriched dissolved organic matter in raw water and treated wastewater effluent. *Water research* **2013,** *47* (8), 2729-2741.

10. Muellner, M. G.; Wagner, E. D.; McCalla, K.; Richardson, S. D.; Woo, Y.-T.; Plewa, M. J., Haloacetonitriles vs. regulated haloacetic acids: are nitrogen-containing DBPs more toxic? *Environmental science & technology* **2007,** *41* (2), 645-651.

11. Zhang, B.; Xian, Q.; Zhu, J.; Li, A.; Gong, T., Characterization, DBPs formation, and mutagenicity of soluble microbial products (SMPs) in wastewater under simulated stressful conditions. *Chemical Engineering Journal* **2015,** *279*, 258-263.

12. Wagner, E. D.; Plewa, M. J., CHO cell cytotoxicity and genotoxicity analyses of disinfection by-products: an updated review. *Journal of Environmental Sciences* **2017,** *58*, 64-76.

13. Hua, G.; Reckhow, D. A., Comparison of disinfection byproduct formation from chlorine and alternative disinfectants. *Water Research* **2007,** *41* (8), 1667-1678.

14. Najm, I.; Trussell, R. R., NDMA formation in water and wastewater. *Journal-American Water Works Association* **2001,** *93* (2), 92-99.

15. Canada, H., Guidelines for Canadian Drinking Water Quality: Trihalomethanes. Environment, F.-P.-T. C. o. D. W. o. t. F.-P.-T. C. o. H. a. t., Ed. 2006; p 67.

16. Canada, H., Guidelines for Canadian drinking water quality—Summary table. *Water and Air Quality Bureau, Healthy Environments and Consumer Safety Branch, Health Canada, Ottawa* **2017**.

17. Chowdhury, S.; Champagne, P.; McLellan, P. J., Models for predicting disinfection byproduct (DBP) formation in drinking waters: a chronological review. *Science of the Total Environment* **2009,** *407* (14), 4189-4206.

18. Singer, P. C.; Reckhow, D. A., Chemical oxidation. *Water quality and treatment* **1999,** *5*.

19. Plewa, M. J.; Wagner, E. D.; Muellner, M. G.; Hsu, K.-M.; Richardson, S. D., Comparative mammalian cell toxicity of N-DBPs and C-DBPs. ACS Publications: 2008.

20. Mitch, W. A.; Sedlak, D. L., Formation of N-nitrosodimethylamine (NDMA) from dimethylamine during chlorination. *Environmental Science & Technology* **2002,** *36* (4), 588-595.

21. Yokose, Y.; Uchida, K.; Nakae, D.; Shiraiwa, K.; Yamamoto, K.; Konishi, Y., Studies of carcinogenicity of sodium chlorite in B6C3F1 mice. *Environ Health Persp* **1987,** *76*, 205-210.

22. McNair, H. M.; Miller, J. M.; Snow, N. H., *Basic gas chromatography*. John Wiley & Sons: 2019.

23. Han, X.; He, X.; Wang, H.; Wang, B.; Wu, B., Fluoro-substituted tetraphenyl–phenyl grafted polysiloxanes as highly selective stationary phases for gas chromatography. *Journal of Chromatography A* **2016,** *1449*, 118-128.

24. Lee, M.; Kuei, J.; Adams, N.; Tarbet, B.; Nishioka, M.; Jones, B.; Bradshaw, J., Polarizable polysiloxane stationary phases for capillary column gas chromatography. *Journal of Chromatography A* **1984,** *302*, 303-318.

25. Kimura, S. Y.; Cuthbertson, A. A.; Byer, J. D.; Richardson, S. D., The DBP exposome: Development of a new method to simultaneously quantify priority

disinfection by-products and comprehensively identify unknowns. *Water research* **2019,** *148*, 324-333.

26. Gross, J. H., *Mass spectrometry: a textbook*. Springer Science & Business Media: 2006.

27. Watson, J. T.; Sparkman, O. D., *Introduction to mass spectrometry: instrumentation, applications, and strategies for data interpretation*. John Wiley & Sons: 2007.

28. Fano, U., On the theory of ionization yield of radiations in different substances. *Physical Review* **1946,** *70* (1-2), 44.

29. Tandem Mass Spectrometry (MS/MS) - MagLab. https://nationalmaglab.org/user-facilities/icr/techniques/tandem-ms (accessed July 06, 2020).

30. Shukla, A. K.; Futrell, J. H., Tandem mass spectrometry: dissociation of ions by collisional activation. *Journal of Mass Spectrometry* **2000,** *35* (9), 1069-1090.

31. Kinani, A.; Olivier, J.; Roumiguières, A.; Bouchonnet, S.; Kinani, S., A sensitive and specific solid-phase extraction–gas chromatography–tandem mass spectrometry method for the determination of 11 haloacetic acids in aqueous samples. *European Journal of Mass Spectrometry* **2018,** *24* (5), 375-383.

32. Cuthbertson, A. A.; Liberatore, H. K.; Kimura, S. Y.; Allen, J. M.; Bensussan, A. V.; Richardson, S. D., Trace analysis of 61 emerging Br-, Cl-, and I-DBPs: New methods to achieve part-per-trillion quantification in drinking water. *Analytical Chemistry* **2020,** *92* (4), 3058-3068.

33. Liu, Y.; Duan, J.; Li, W.; Lai, Q.; Saint, C. P.; Mulcahy, D., Determination of volatile disinfection byproducts in water by gas chromatography–triple quadrupole mass spectrometry. *Analytical Letters* **2015,** *48* (1), 188-203.

34. Roumiguières, A.; Kinani, A.; Bouchonnet, S.; Kinani, S., Development and validation of a multiclass method for the determination of organohalogen disinfectant by-products in water samples using solid phase extraction and gas chromatography-tandem mass spectrometry. *Journal of Chromatography A* **2018,** *1579*, 89-98.

35. Richardson, S. D.; Ternes, T. A., Water analysis: emerging contaminants and current issues. *Analytical chemistry* **2011,** *83* (12), 4614-4648.

36. Costet, N.; Villanueva, C.; Jaakkola, J.; Kogevinas, M.; Cantor, K.; King, W.; Lynch, C.; Nieuwenhuijsen, M.; Cordier, S., Water disinfection by-products and bladder cancer: is there a European specificity? A pooled and meta-analysis of European case–control studies. *Occupational and environmental medicine* **2011,** *68* (5), 379-385.

37. Grazuleviciene, R.; Kapustinskiene, V.; Vencloviene, J.; Buinauskiene, J.; Nieuwenhuijsen, M. J., Risk of congenital anomalies in relation to the uptake of trihalomethane from drinking water during pregnancy. *Occupational and Environmental Medicine* **2013,** *70* (4), 274-282.

38. Horton, B. J.; Luben, T. J.; Herring, A. H.; Savitz, D. A.; Singer, P. C.; Weinberg, H. S.; Hartmann, K. E., The effect of water disinfection by-products on pregnancy outcomes in two southeastern US communities. *Journal of occupational and environmental medicine/American College of Occupational and Environmental Medicine* **2011,** *53* (10), 1172.

39. Nieuwenhuijsen, M. J.; Dadvand, P.; Grellier, J.; Martinez, D.; Vrijheid, M., Environmental risk factors of pregnancy outcomes: a summary of recent meta-analyses of epidemiological studies. *Environmental health* **2013,** *12* (1), 6.

40. Righi, E.; Bechtold, P.; Tortorici, D.; Lauriola, P.; Calzolari, E.; Astolfi, G.; Nieuwenhuijsen, M. J.; Fantuzzi, G.; Aggazzotti, G., Trihalomethanes, chlorite, chlorate in drinking water and risk of congenital anomalies: a population-based case-control study in Northern Italy. *Environmental Research* **2012,** *116*, 66-73.

41. Smith, R. B.; Edwards, S. C.; Best, N.; Wright, J.; Nieuwenhuijsen, M. J.; Toledano, M. B., Birth weight, ethnicity, and exposure to trihalomethanes and haloacetic acids in drinking water during pregnancy in the Born in Bradford cohort. *Environ Health Persp* **2016,** *124* (5), 681-689.

42. Villanueva, C. M.; Cantor, K. P.; Cordier, S.; Jaakkola, J. J.; King, W. D.; Lynch, C. F.; Porru, S.; Kogevinas, M., Disinfection byproducts and bladder cancer: a pooled analysis. *Epidemiology* **2004**, 357-367.

43. Villanueva, C. M.; Cantor, K. P.; Grimalt, J. O.; Malats, N.; Silverman, D.; Tardon, A.; Garcia-Closas, R.; Serra, C.; Carrato, A.; Castano-Vinyals, G., Bladder cancer and exposure to water disinfection by-products through ingestion, bathing, showering, and swimming in pools. *American journal of epidemiology* **2007,** *165* (2), 148-156.

44. Villanueva, C. M.; Fernandez, F.; Malats, N.; Grimalt, J. O.; Kogevinas, M., Meta-analysis of studies on individual consumption of chlorinated drinking water and bladder cancer. *Journal of Epidemiology & Community Health* **2003,** *57* (3), 166-173.

45. Waller, K.; Swan, S. H.; DeLorenze, G.; Hopkins, B., Trihalomethanes in drinking water and spontaneous abortion. *Epidemiology* **1998**, 134-140.

46. Wright, J. M.; Evans, A.; Kaufman, J. A.; Rivera-Núñez, Z.; Narotsky, M. G., Disinfection by-product exposures and the risk of specific cardiac birth defects. *Environ Health Persp* **2017,** *125* (2), 269-277.

47. Richardson, S. D.; Plewa, M. J., To regulate or not to regulate? What to do with more toxic disinfection by-products? *Journal of Environmental Chemical Engineering* **2020**, 103939.

48. Rice, J.; Westerhoff, P., Spatial and temporal variation in de facto wastewater reuse in drinking water systems across the USA. *Environmental Science & Technology* **2015,** *49* (2), 982-989.

49. Rice, J.; Wutich, A.; Westerhoff, P., Assessment of de facto wastewater reuse across the US: trends between 1980 and 2008. *Environmental science & technology* **2013,** *47* (19), 11099-11105.

50. Li, X.-F.; Mitch, W. A., Drinking water disinfection byproducts (DBPs) and human health effects: multidisciplinary challenges and opportunities. ACS Publications: 2018.

51. Marron, E. L.; Mitch, W. A.; Gunten, U. v.; Sedlak, D. L., A tale of two treatments: the multiple barrier approach to removing chemical contaminants during potable water reuse. *Accounts Chem. Res.* **2019,** *52* (3), 615-622.

52. Alexandrou, L.; Meehan, B. J.; Jones, O. A., Regulated and emerging disinfection by-products in recycled waters. *Science of the Total Environment* **2018,** *637*, 1607-1616.

53. Chuang, Y.-H.; Mitch, W. A., Effect of ozonation and biological activated carbon treatment of wastewater effluents on formation of N-nitrosamines and halogenated disinfection byproducts. *Environmental science & technology* **2017,** *51* (4), 2329-2338.

54. Chuang, Y.-H.; Parker, K. M.; Mitch, W. A., Development of predictive models for the degradation of halogenated disinfection byproducts during the UV/H2O2 advanced oxidation process. *Environmental science & technology* **2016,** *50* (20), 11209-11217.

55. Chuang, Y.-H.; Szczuka, A.; Mitch, W. A., Comparison of toxicity-weighted disinfection byproduct concentrations in potable reuse waters and conventional drinking waters as a new approach to assessing the quality of advanced treatment train waters. *Environmental science & technology* **2019,** *53* (7), 3729-3738.

56. Chuang, Y.-H.; Szczuka, A.; Shabani, F.; Munoz, J.; Aflaki, R.; Hammond, S. D.; Mitch, W. A., Pilot-scale comparison of microfiltration/reverse osmosis and ozone/biological activated carbon with UV/hydrogen peroxide or UV/free chlorine AOP treatment for controlling disinfection byproducts during wastewater reuse. *Water research* **2019,** *152*, 215-225.

57. Doederer, K.; Gernjak, W.; Weinberg, H. S.; Farré, M. J., Factors affecting the formation of disinfection by-products during chlorination and chloramination of secondary effluent for the production of high quality recycled water. *Water Research* **2014,** *48*, 218-228.

58. Krasner, S. W.; Westerhoff, P.; Chen, B.; Rittmann, B. E.; Amy, G., Occurrence of disinfection byproducts in United States wastewater treatment plant effluents. *Environmental Science & Technology* **2009,** *43* (21), 8320-8325.

59. Linge, K. L.; Blythe, J. W.; Busetti, F.; Blair, P.; Rodriguez, C.; Heitz, A., Formation of halogenated disinfection by-products during microfiltration and reverse osmosis treatment: implications for water recycling. *Separation and Purification Technology* **2013,** *104*, 221-228.

60. Zeng, T.; Plewa, M. J.; Mitch, W. A., N-Nitrosamines and halogenated disinfection byproducts in US Full Advanced Treatment trains for potable reuse. *Water research* **2016,** *101*, 176-186.

61. Dong, S.; Page, M. A.; Massalha, N.; Hur, A.; Hur, K.; Bokenkamp, K.; Wagner, E. D.; Plewa, M. J., Toxicological comparison of water, wastewaters, and processed wastewaters. *Environmental science & technology* **2019,** *53* (15), 9139-9147.

62. Du, Y.; Wang, W.-L.; He, T.; Sun, Y.-X.; Lv, X.-T.; Wu, Q.-Y.; Hu, H.-Y., Chlorinated effluent organic matter causes higher toxicity than chlorinated natural organic matter by inducing more intracellular reactive oxygen species. *Science of The Total Environment* **2020,** *701*, 134881.

63. Richardson, S. D.; Kimura, S. Y., Water analysis: emerging contaminants and current issues. *Analytical chemistry* **2016,** *88* (1), 546-582.

64. Richardson, S. D.; Kimura, S. Y., Water analysis: emerging contaminants and current issues. *Analytical Chemistry* **2019,** *92* (1), 473-505.

65. Richardson, S. D.; Ternes, T. A., Water analysis: emerging contaminants and current issues. *Analytical chemistry* **2014,** *86* (6), 2813-2848.

66. Richardson, S. D.; Ternes, T. A., Water analysis: emerging contaminants and current issues. *Analytical chemistry* **2018,** *90* (1), 398-428.

67. Bougeard, C. M.; Goslan, E. H.; Jefferson, B.; Parsons, S. A., Comparison of the disinfection by-product formation potential of treated waters exposed to chlorine and monochloramine. *Water research* **2010,** *44* (3), 729-740.

68. Carter, R. A.; Liew, D. S.; West, N.; Heitz, A.; Joll, C. A., Simultaneous analysis of haloacetonitriles, haloacetamides and halonitromethanes in chlorinated waters by gas chromatography-mass spectrometry. *Chemosphere* **2019,** *220*, 314-323.

69. Krasner, S. W.; Weinberg, H. S.; Richardson, S. D.; Pastor, S. J.; Chinn, R.; Sclimenti, M. J.; Onstad, G. D.; Thruston, A. D., Occurrence of a new generation of disinfection byproducts. *Environmental science & technology* **2006,** *40* (23), 7175-7185.

70. Weinberg, H. S.; Krasner, S. W.; Richardson, S. D.; Thruston Jr, A., The occurrence of disinfection by-products (DBPs) of health concern in drinking water: results of a nationwide DBP occurrence study. *National Exposure Research Laboratory, Office of Research and Development, US Environmental Protection Agency* **2002**.

71. Chuang, Y.-H.; Tung, H.-h., Formation of trichloronitromethane and dichloroacetonitrile in natural waters: precursor characterization, kinetics and interpretation. *Journal of Hazardous Materials* **2015,** *283*, 218-226.

72. Stone, P.; Glauner, T.; Kuhlmann, F.; Schlabach, T.; Miller, K., New dynamic MRM mode improves data quality and triple quad quantification in complex analyses. *Agilent publication* **2009**.

73. Nichols, C.; Zekavat, B.; Batoon, P., Instrument Detection Limit at Ultrashort Dwell Times Demonstrated on the Agilent 6495C Triple Quadrupole LC/MS.

74. Kirchner, M.; Matisová, E.; Hrouzková, S.; de Zeeuw, J., Possibilities and limitations of quadrupole mass spectrometric detector in fast gas chromatography. *Journal of Chromatography A* **2005,** *1090* (1-2), 126-132.

75. Sargent, M., Guide to achieving reliable quantitative LC-MS measurements. *RSC analytical methods committee* **2013**.

76. Summers, R. S.; Hooper, S. M.; Shukairy, H. M.; Solarik, G.; Owen, D., Assessing DBP yield: uniform formation conditions. *Journal-American Water Works Association* **1996,** *88* (6), 80-93.

77. Kimura, S. Y.; Komaki, Y.; Plewa, M. J.; Mariñas, B. J., Chloroacetonitrile and N, 2-dichloroacetamide formation from the reaction of chloroacetaldehyde and monochloramine in water. *Environmental science & technology* **2013,** *47* (21), 12382-12390.

78. Kimura, S. Y.; Vu, T. N.; Komaki, Y.; Plewa, M. J.; Mariñas, B. J., Acetonitrile and N-chloroacetamide formation from the reaction of acetaldehyde and monochloramine. *Environmental science & technology* **2015,** *49* (16), 9954-9963.

79. Association, A. P. H.; Association, A. W. W.; Federation, W. P. C.; Federation, W. E., *Standard methods for the examination of water and wastewater*. American Public Health Association.: 1915; Vol. 2.

80. Kimura, S. Y.; Zheng, W.; Hipp, T. N.; Allen, J. M.; Richardson, S. D., Total organic halogen (TOX) in human urine: A halogen-specific method for human exposure studies. *Journal of Environmental Sciences* **2017,** *58*, 285-295.

81. Doederer, K.; Farré, M. J.; Pidou, M.; Weinberg, H. S.; Gernjak, W., Rejection of disinfection by-products by RO and NF membranes: influence of solute properties and operational parameters. *J. Membr. Sci.* **2014,** *467*, 195-205.

82. Huang, H.; Chen, B.-Y.; Zhu, Z.-R., Formation and speciation of haloacetamides and haloacetonitriles for chlorination, chloramination, and chlorination followed by chloramination. *Chemosphere* **2017,** *166*, 126-134.

83. Huang, H.; Wu, Q.-Y.; Hu, H.-Y.; Mitch, W. A., Dichloroacetonitrile and dichloroacetamide can form independently during chlorination and chloramination of drinking waters, model organic matters, and wastewater effluents. *Environmental science & technology* **2012,** *46* (19), 10624-10631.

84. Kozari, A.; Paloglou, A.; Voutsa, D., Formation potential of emerging disinfection by-products during ozonation and chlorination of sewage effluents. *Science of The Total Environment* **2020,** *700*, 134449.

85. McCurry, D. L.; Quay, A. N.; Mitch, W. A., Ozone promotes chloropicrin formation by oxidizing amines to nitro compounds. *Environmental science & technology* **2016,** *50* (3), 1209-1217.

86. Yang, X.; Peng, J.; Chen, B.; Guo, W.; Liang, Y.; Liu, W.; Liu, L., Effects of ozone and ozone/peroxide pretreatments on disinfection byproduct formation during subsequent chlorination and chloramination. *Journal of Hazardous Materials* **2012,** *239*, 348-354.

87. Chen, M.; Cooper, V.; Deng, J.; Amatya, P.; Ambrus, D.; Dong, S.; Stalker, N.; Nadeau-Bonilla, C.; Patel, J., Occurrence of pharmaceuticals in Calgary's wastewater and related surface water. *Water Environ. Res.* **2015,** *87* (5), 414-424.

88. Chen, M.; Ohman, K.; Metcalfe, C.; Ikonomou, M. G.; Amatya, P. L.; Wilson, J., Pharmaceuticals and endocrine disruptors in wastewater treatment effluents and in the water supply system of Calgary, Alberta, Canada. *Water Quality Research Journal* **2006,** *41* (4), 351-364.

89. Song, H.; Addison, J. W.; Hu, J.; Karanfil, T., Halonitromethanes formation in wastewater treatment plant effluents. *Chemosphere* **2010,** *79* (2), 174-179.

90. Yang, X.; Shang, C.; Shen, Q.; Chen, B.; Westerhoff, P.; Peng, J.; Guo, W., Nitrogen origins and the role of ozonation in the formation of haloacetonitriles and halonitromethanes in chlorine water treatment. *Environmental science & technology* **2012,** *46* (23), 12832-12838.

91. Bichsel, Y.; Von Gunten, U., Oxidation of iodide and hypoiodous acid in the disinfection of natural waters. *Environmental science & technology* **1999,** *33* (22), 4040-4045.

92. Bichsel, Y.; Von Gunten, U., Formation of iodo-trihalomethanes during disinfection and oxidation of iodide-containing waters. *Environmental Science & Technology* **2000,** *34* (13), 2784-2791.

93. Allard, S.; Charrois, J. W.; Joll, C. A.; Heitz, A., Simultaneous analysis of 10 trihalomethanes at nanogram per liter levels in water using solid-phase microextraction and gas chromatography mass-spectrometry. *Journal of Chromatography A* **2012,** *1238*, 15-21.

94. Lavonen, E. E.; Gonsior, M.; Tranvik, L. J.; Schmitt-Kopplin, P.; Kohler, S. J., Selective Chlorination of Natural Organic Matter: Identification of Previously Unknown Disinfection Byproducts. *Environmental Science & Technology* **2013,** *47* (5), 2264-2271.